

Part 2: Literature overview

Chapter 2: Metal carbenes in homogeneous alkene metathesis: computational investigations

2.1 Motivation

An investigation and overview were done only on the theoretical and computational investigations of alkene metathesis. To my knowledge no known overview has been done on this theme. The literature search was also done to verify the current state of modelling of alkene metathesis and whether any other study has considered the detailed use of any chemical reactivity indicators. The overview comprises five main parts, namely: relevant historical moments in alkene metathesis, reaction mechanism of alkene metathesis, properties of transition metal carbene complexes, theoretical treatment of the four main types of metal carbenes used in alkene metathesis and computational investigations of the four main types of metal carbenes in alkene metathesis.

2.2 Review article

Metal carbenes in homogeneous alkene metathesis: computational investigations

Keywords

Metathesis
Transition metal carbene complexes
Molecular modeling

Contents

1. Introduction to alkene metathesis	12
2. Relevant historical moments in alkene metathesis	13
3. Reaction mechanism of alkene metathesis	16
4. Properties of transition metal carbene complexes	17
4.1 Nature of the bonding in transition metal carbene complexes	17
4.2 Classification of metal carbenes	19
4.2.1 Schrock-type metal carbene	22
4.2.2 Fischer-type metal carbene	23
4.2.3 Ruthenium metal carbene	25
5. Theoretical treatment of the four main types of metal carbenes used in alkene metathesis	25
6. Computational investigations of the four main types of metal carbenes in alkene metathesis	29
6.1 Fischer-type metal carbene catalysts	29
6.2 Tebbe-type metal carbene catalysts	29
6.3 Grubbs-type metal carbene catalysts	31
6.4 Schrock-type metal carbene catalysts	44
7. Summary	55

1. Introduction

“The alkene metathesis reaction is one of the most original and unusual transformations in chemistry. Remarkably, the strongest bond in the alkene, the C=C

double bond, is broken during the reaction” [1]. Alkene metathesis has come a long way since the first observation by Eleuterio in 1956 [2]. Some of the industrial applications include routes to “important petrochemicals, polymers, oleochemicals and speciality chemicals”, with the most vital applications in the field of petrochemicals the olefins conversion technology (OCT) process and the Shell higher olefins process (SHOP) [3].

Chauvin’s metal carbene mechanism (Scheme 1) paved the way for researchers to develop new catalysts. With the discovery of metal carbenes being able to catalyze the alkene metathesis reaction, the possibility of using well-defined homogeneous catalysts became a reality. From the first used Fischer-type metal carbenes [4-6] to the discovery of the highly active Schrock- [7] and Grubbs-type [8] metal carbenes these carbenes proved themselves as powerful catalysts for alkene metathesis.

The advent of computational chemistry further opened opportunities for elucidating and understanding the alkene metathesis mechanism. With the modeling tools and computational power now available, we are able to design and develop new catalysts in a cost-effective way before experimental testing. This paper gives an overview of computational metathesis, specifically focusing on transition metal carbenes as catalysts and the four main types of metal carbenes used in alkene metathesis.

2. Relevant historical moments in alkene metathesis

1956 Eleuterio observed metathesis for the first time. He found a propene-ethene copolymer from a propylene feed over a molybdenum-alumina catalyst. The products were a mixture of propene, ethene and 1-butene [2].

1967 Calderon *et al.* [9] at “Goodyear Tire & Rubber” in Ohio found that products form from the breaking and rearranging of an alkene’s double bond. They coined the reaction “*olefin metathesis*”. Other researchers came to a similar

conclusion at about the same time [2].

1971 Chauvin and Herisson [10] proposed that alkene metathesis is initiated by a metal carbene that reacts with an alkene to form a metallacyclobutane intermediate.

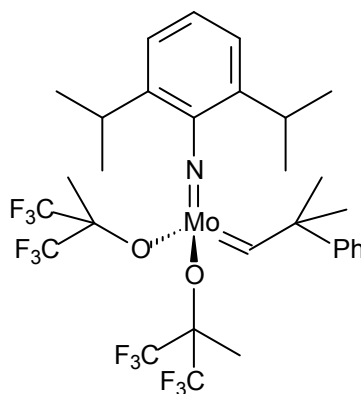
1974 Casey and Burkhardt [4] demonstrated for the first time that a metal carbene, (diphenylcarbene)pentacarbonyltungsten, reacts with an alkene, isobutene, to form as main product a new alkene, 1,1-diphenylethene.

1975 The work of Katz and McGinnis [5] was the first to clearly confirm the metal carbene mechanism for the alkene metathesis reaction.

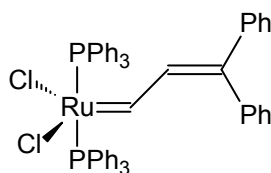
1976 Katz *et al.* [6] reported the first use of an isolatable metal carbene complex, (diphenylcarbene)-pentacarbonyltungsten, to initiate the metathesis of unsymmetrically substituted ethene.

1980 Schrock [11] reported metathesis of *cis*-2-pentene in the presence of the $M(\text{CHCMe}_3)(\text{OCMe}_3)_2(\text{PR}_3)\text{Cl}$ -type complexes [$M = \text{Nb}$ or Ta , $R = \text{Me}$, Et].

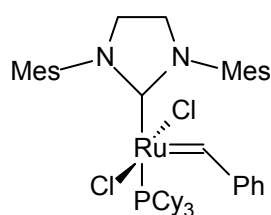
1990 Schrock [7] replaced *in situ* generated catalyst systems with a well-defined molybdenum precatalyst



1992 Grubbs [8] synthesized a ruthenium carbene.



2000 Grubbs [12] prepared an *in situ* highly active N-heterocyclic carbene coordinated catalyst.



2004 Comprehensive DFT study on the mechanism of the ruthenium catalyzed alkene metathesis reaction by Adlhart and Chen [13].

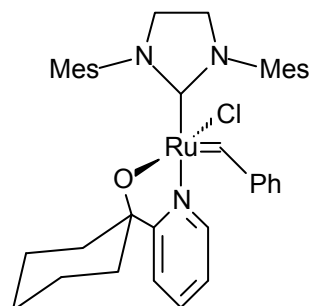
2005 Chauvin, Grubbs and Schrock received the Nobel Prize in Chemistry.

2006 Grubbs and Hong [14] prepared a highly active water-soluble alkene metathesis catalyst.

2006 Grubbs [15] developed a standard system of characterization for alkene metathesis catalysts.

2006 Jordaan *et al.* [16] did a DFT study on the complete catalytic cycle of the reaction of 1-octene catalyzed by the Grubbs first generation catalyst.

2007 Jordaan and Vosloo [17] synthesized a ruthenium catalyst with a chelating pyridinyl-alcoholato ligand for application in linear alkene metathesis.



2008 Schrock [18] reported highly efficient molybdenum-based catalysts for enantioselective alkene metathesis.

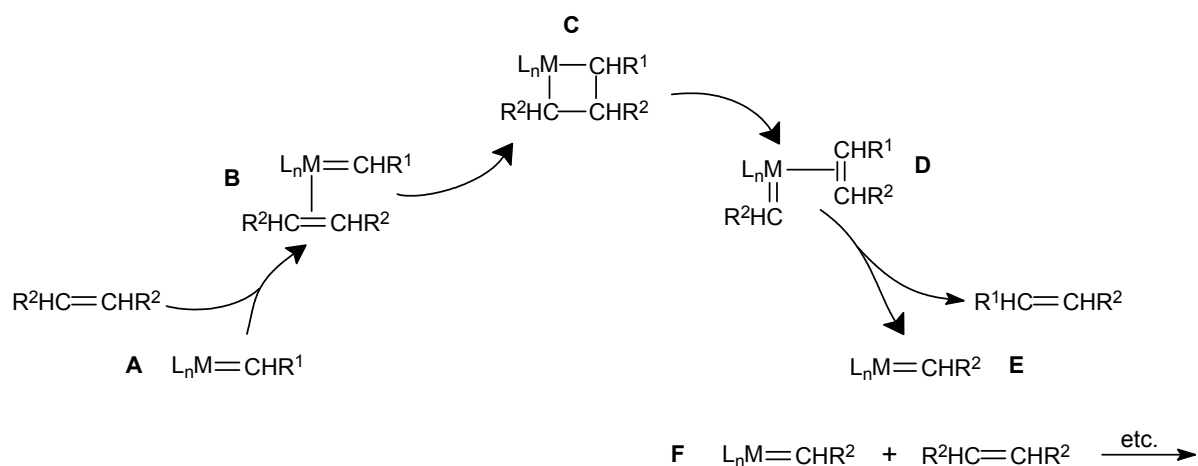
2009 Marx, Jordaan and Vosloo [19] did a DFT study on the complete catalytic cycle of the reaction of 1-octene catalyzed by the Phobcat precatalyst.

2009 Ibrahim, Schrock and Hoveyda [20] presented the first highly Z- and enantioselective class of ring-opening/ cross metathesis reactions.

2011 Endo and Grubbs [21] developed chelated ruthenium catalysts for Z-selective metathesis.

3. Reaction mechanism of alkene metathesis

The currently accepted metal carbene mechanism [22] is outlined in Scheme 1.



Scheme 1 Reaction scheme of the alkene metathesis metal carbene mechanism.

The mechanism consists out of the coordination of an alkene (**B**) to the metal of the metal carbene (**A**); a [2+2]-cycloaddition between the metal carbene and the alkene to form a metallacyclobutane intermediate (**C**); the breaking of the metallacyclobutane intermediate to form a carbene and an alkene (**D**); the replacement of the coordinated alkene with a new alkene to restart the cycle (**F**) [22].

4. Properties of transition metal carbene complexes

4.1 Nature of the bonding in transition metal carbene complexes

The nature of the bonding in transition metal carbene complexes plays a key role in the properties and subsequent classification of metal carbenes. The schematic description of the bonding in a metal carbene complex (Fig. 1) shows the situation for a complex ML_n for $n = 4-9$ where there are n M-L σ -bonding orbitals and $(9 - n)$ non-bonding d orbitals. 18 electrons are required to fill the bonding and non-bonding levels [1].

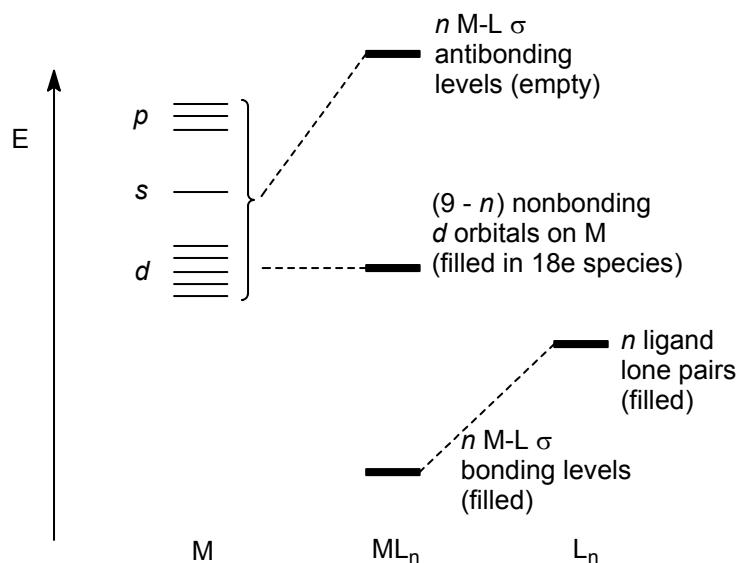


Fig. 1. Schematic description of the bonding in a metal complex. The thick horizontal lines represent several orbitals somewhat spread out in energy, depending on the exact nature of the complex [1],[23].

Bonding takes place between the metal orbitals and the ligand orbitals. Metal orbitals, being less electronegative than ligand orbitals, are placed higher in energy [23]. A simplified diagram of the interaction of two orbitals, e.g. a metal orbital and a ligand orbital, is given in Fig. 2. Orbitals must have the same symmetry to be able to interact with one another.

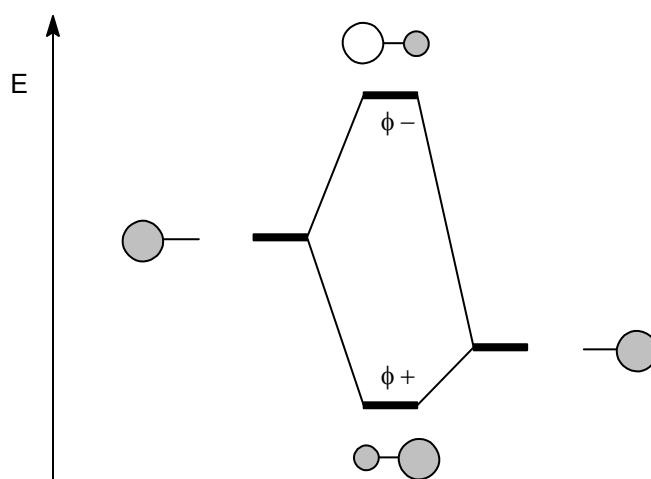


Fig. 2. Interaction diagram for two orbitals with different energies [23],[24].

As can be seen from Fig. 1 and 2 the bonding molecular orbitals are concentrated on the ligand orbitals (lowest energy orbitals) and the antibonding molecular orbitals are concentrated on the metal orbitals. Non-bonding orbitals are localized on the metal centre [23]. For ligand orbitals to be able to interact with the metal orbitals the energy value of the orbitals must be close and the overlap of the orbitals must be substantial [23].

4.2 Classification of metal carbenes

The classification of carbenes is, at the fundamental level, determined by the nature of the transition metal-carbene bond [25]. Carbenes can be either formed by spin triplet fragments or by spin singlet fragments [1],[22],[25],[26] (Fig. 3). The single valence bond orbitals of the π electrons and the σ electrons for an example triplet and singlet carbene are shown in Fig. 4 [26]. For the triplet carbene it is evident that one π electron and one σ electron are localized on each centre. In the case of the singlet carbene both π electrons are located primarily on the metal and both σ electrons are located on the carbene [26].

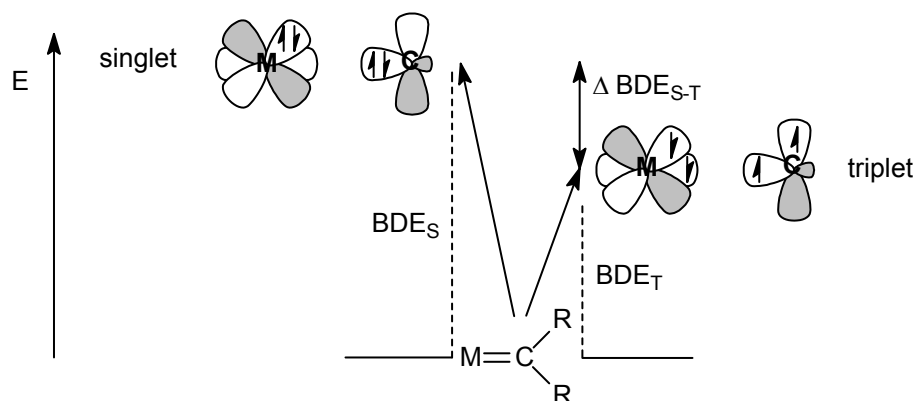


Fig. 3. Singlet and triplet cleavage of the M=C bond [25].

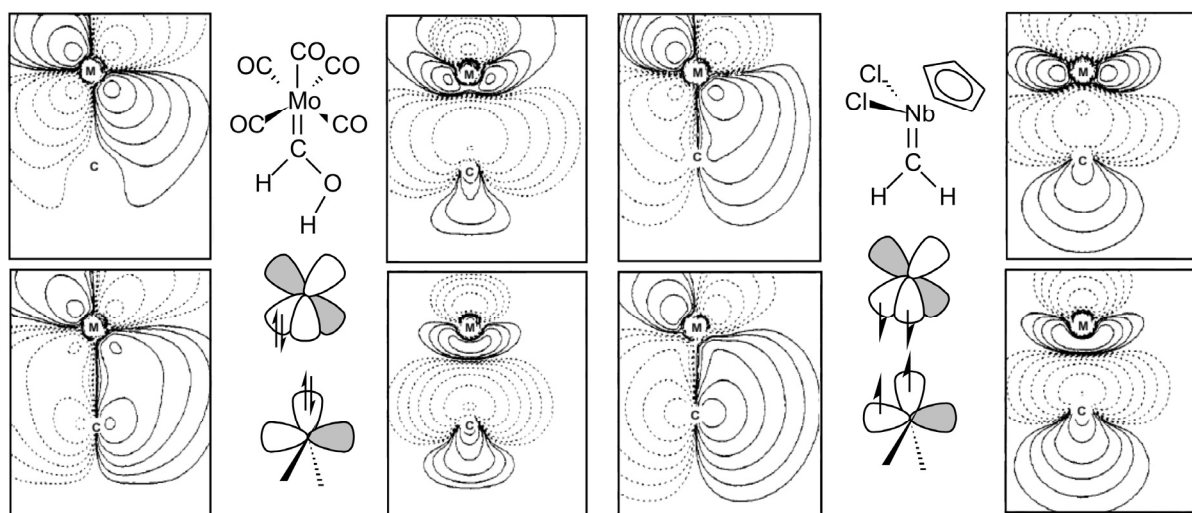


Fig. 4. Valence bond orbitals of $(\text{CO})_5\text{Mo}=\text{CH}(\text{OH})$ (left) and $\text{CpCl}_2\text{Nb}=\text{CH}_2$ (right). Each map is the electron density of one electron and is in the plane of the π bond. The π electrons are in the left columns and σ electrons are in the right columns [26].

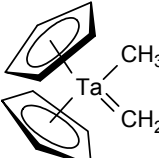
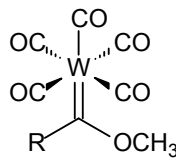
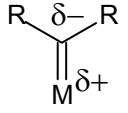
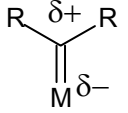
Carbenes can show either electrophilic or nucleophilic activity [27] depending on whether the two electrons on the carbon atom are paired (singlet) or unpaired (triplet) [22],[24]. Those that are nucleophilic at the carbene atom are called Schrock-type complexes [22],[24],[27]. Schrock [28] reported the first example of such a complex in 1974. Metal carbenes that are electrophilic at the carbene carbon are called Fischer-type complexes [22],[24],[27]. Fischer [29] reported the first example of such a complex in 1964. Typical reactions of nucleophilic carbenes include carbonyl alkylation and alkene metathesis. Electrophilic carbenes undergo alkene cyclopropanation, C-H insertions and ylid forming reactions [22].

The activity of metal carbenes is furthermore strongly influenced by the electronic properties of their substituents. Metal carbenes can be stabilized by complexation of an atom with a lone pair (e.g. O, N, or S) directly bonded to the carbene carbon. The nature of the subsequent molecular orbitals of carbenes allows the metal carbenes to act as σ -donors and π -acceptors. The ability of the metal to accept σ -electrons from the carbene carbon atom and the capacity of the metal for π -back bonding in the empty p-orbitals of the carbene carbon atom are important for the activity of the metal carbene complexes [27]. Metallic fragments that are good σ -acceptors and good π -

donors form strong carbon-metal bonding, with typical Schrock-type carbenes forming part of this group. Weak σ -acceptor and good π -donor metallic fragments also lead to nucleophilic metal carbenes but with weaker carbon-metal bonding. On the other hand electrophilic Fischer-type carbenes have good σ -acceptor and weak π -donor metallic fragments. In the case of weak σ -acceptor and weak π -donor metallic fragments the interaction between the metal and the carbene is very weak and they are highly reactive complexes [27].

As more metal carbenes are studied, the classification becomes more complex. The metal carbene complexes cannot be classified anymore as absolute Schrock or absolute Fischer. The varieties of structures and activities must rather be seen as points along a continuum. Differences in electronic ground states of the carbene and metal fragments define the extremes of the continuum. Table 1 shows a summary of the traditional Schrock- and Fischer-type metal carbene complexes [22].

Table 1 Characteristics of traditional Schrock- and Fischer-type metal carbene complexes [22],[24],[30]

	Traditional Schrock-type metal carbene (alkylidene)	Traditional Fischer-type metal carbene
Example:		
Ground state:	triplet	singlet
Typical metals:	higher oxidation state, early transition metals such as Ti(IV), Ta(V), etc. [31]	lower oxidation state, later transition metals like W(0), Cr(0), etc. [31]
Typical ligands on M:	Cl, Cp, alkyl	good π -acceptors, e.g. CO
Typical carbene substituents:	alkyl, aryl, H	good π -donors, e.g. OR, NR ₂
Character of carbene carbon:	nucleophilic 	electrophilic 
Metal-carbon bond order:	2	1-2
Bonding interactions:	M-C covalent σ + M-C covalent π	C \rightarrow M dative σ + M \rightarrow C π -back bonding + heteroatom π -donor
Trends:	metal \rightarrow carbon π -back bonding decreases \rightarrow bond order decreases \rightarrow reactivity of carbene carbon changes from nucleophilic to electrophilic \rightarrow	

4.2.1 Schrock-type metal carbene

Schrock-type metal carbenes are usually high valent complexes with less than 18 valence electrons [27]. Early transition metals with high oxidation states form part of the group. The metal-carbene bonds are normal covalent bonds between open-shell

metal fragments and triplet carbenes [32]. Good substituents for Schrock-type metal carbenes are groups that are not π -donors, for example alkyl groups [30]. π -Donors will cause the destabilization of metal carbene bond, because of the electron repellent effect. Thus, for carbenes $L_nM=CR_2$, the L ligand is a non- π -acceptor and the R substituents are non- π -donors [1]. In the molecular orbital diagram the HOMO is mainly localized on the carbon and the LUMO is mainly localized on the metal (Fig. 5) [24],[33]. The activity of Schrock-type metal carbenes is controlled by the frontier orbitals [33],[34].

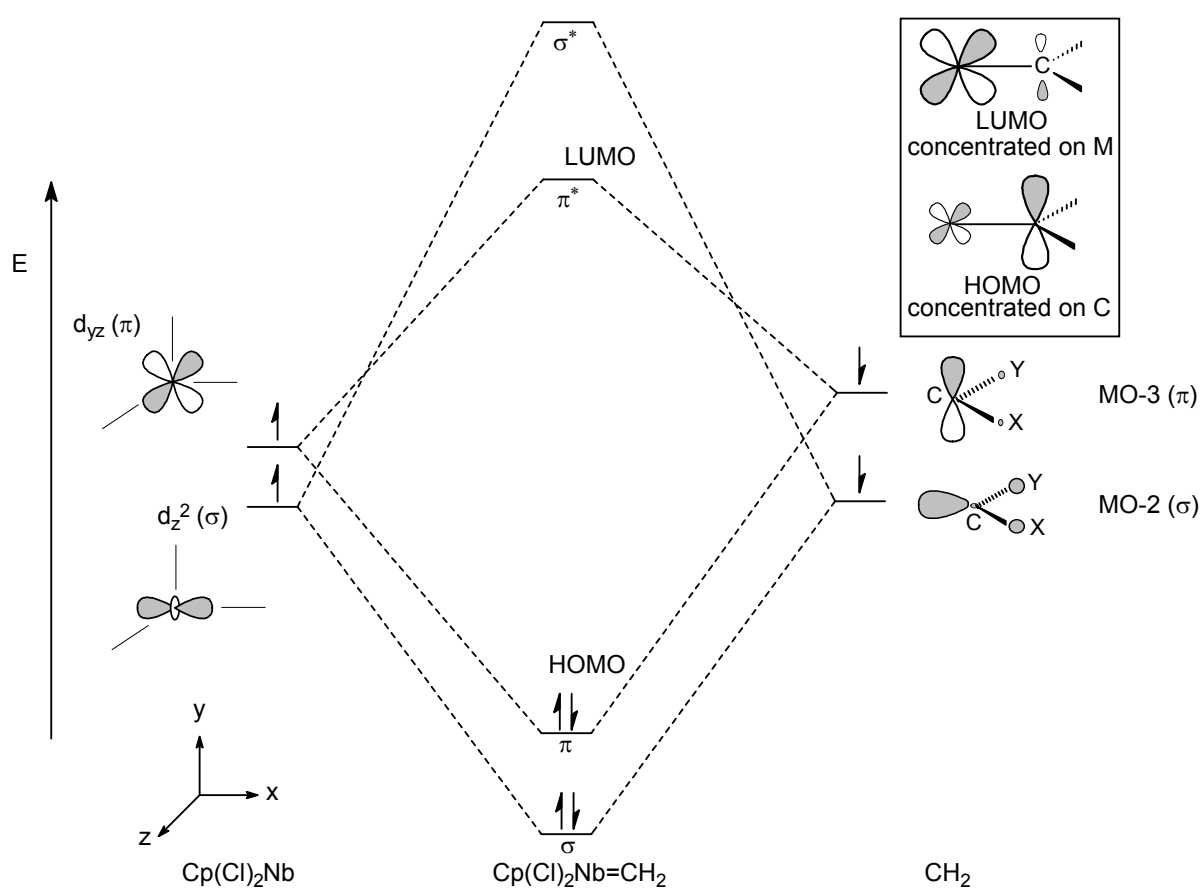


Fig. 5. Partial molecular orbital diagram of a Schrock-type metal carbene complex with X,Y = H, alkyl [24],[35].

4.2.2 Fischer-type metal carbene

Fischer-type metal carbenes are typically low valent, 18-electron complexes [27]. The metal-carbene bonds are due to donor-acceptor interactions between the metal

fragment and singlet carbenes [32]. Fischer-type metal carbenes are stabilized by a major π -contribution by both the substituents and the metal into the empty p-orbital. Good π -back bonding of the metal to the empty p-orbital of the carbene is critical. Thus, for carbenes $L_nM=CR_2$, the L ligand is a π -acceptor and the R substituents are π -donors [1]. Early transition-/ high oxidation state metals that are weak π -donors destabilize Fischer carbenes. Later transition-/ low oxidation state metal complexes are much more stable [30]. In the molecular orbital diagram the antibonding LUMO is mainly localized on the carbon and the HOMO is mainly localized on the metal (Fig. 6) [24]. This is exactly the opposite of the situation of Schrock-type metal carbenes. The activity of Fischer-type metal carbenes is, just like the Schrock-type metal carbenes, controlled by the frontier orbitals [34], [33].

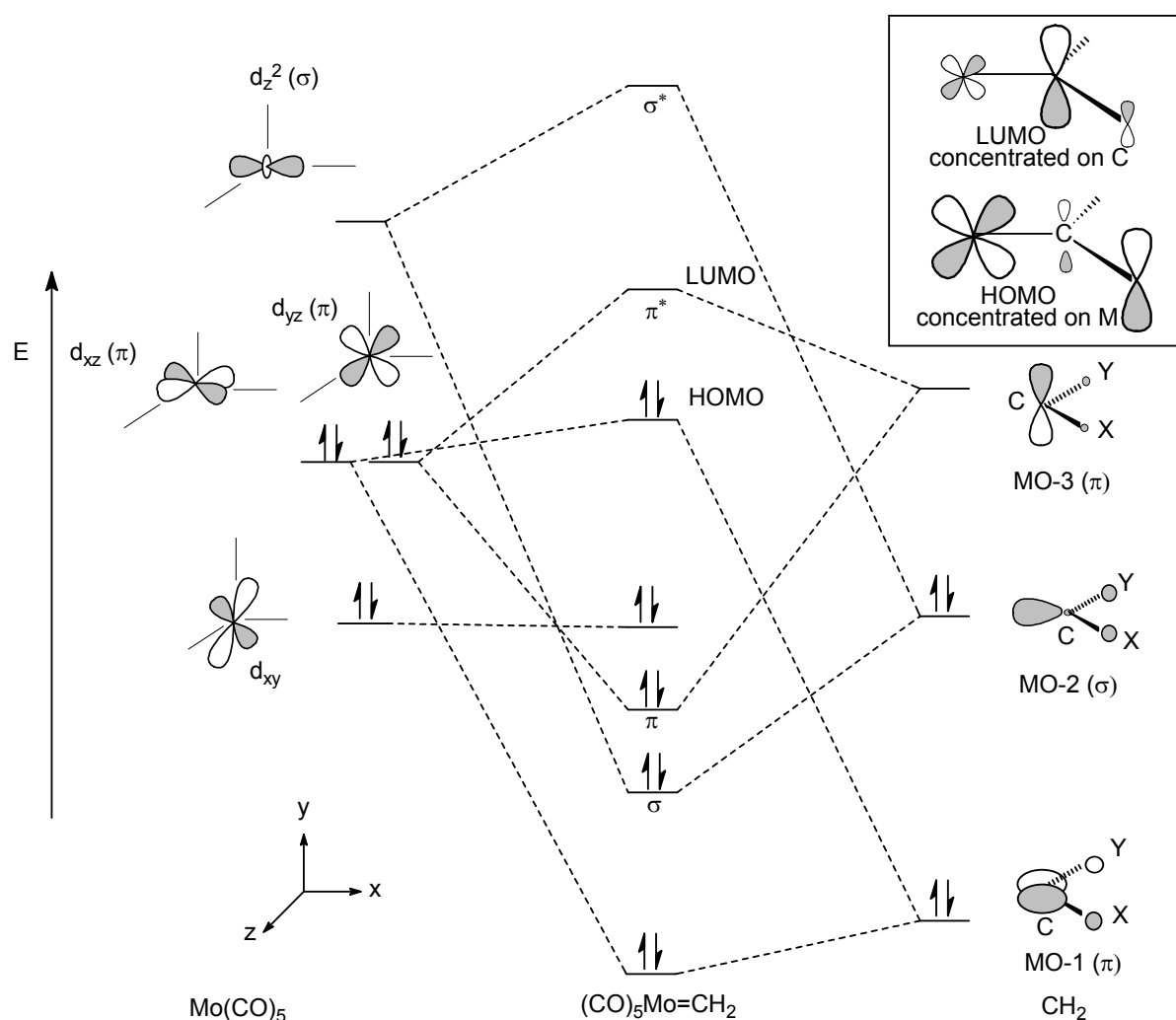


Fig. 6. Partial molecular orbital diagram of a Fischer-type carbene complex with X, Y = Cl, O, N, S [24],[35].

4.2.3 Ruthenium metal carbene

Ruthenium metal carbenes are the main alkene metathesis catalysts used in synthesis today. Classification of the ruthenium metal carbenes as a Schrock- or Fischer-type carbene is central to understanding the activity of these carbenes. In a study done by Occhipinti and Jensen [25] they established that the ruthenium metal carbenes have characteristic properties similar to those of the Schrock-type metal carbenes and can be viewed as an addition to that class. Fig. 7 shows the carbenes evaluated in the study.

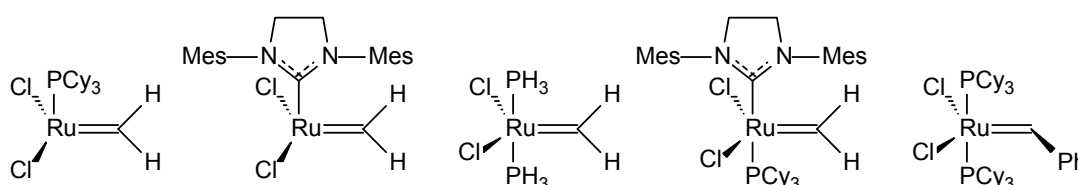


Fig. 7. Ruthenium metal carbenes investigated with Cy = cyclohexyl and Mes = $C_6H_2Me_3$ [25].

In all cases the carbenes have a metal fragment and a carbene fragment in spin triplet ground states with a covalent $TM=C$ bond. Furthermore, the compounds also possess a relatively large triplet-singlet energy gap [25]. The biggest difference between the Schrock-type carbenes and the ruthenium carbenes could be found in their electrophilic/ nucleophilic character. Thus Schrock carbenes were classified as nucleophilic covalent, whereas ruthenium carbenes were classified as electrophilic covalent [25].

5. Theoretical treatment of the four main types of metal carbenes used in alkene metathesis

Fig. 8 and Fig. 9 give a concise account of the theoretical treatment of the four main types of metal carbenes. The precatalyst and catalyst species are tabulated separately for comparison. It is interesting to note that the active catalyst species of the Grubbs- and Schrock-type carbenes have the same tetrahedral molecular geometry around the central metal atom. Furthermore, both active catalyst are 14-electron species therefore

alluding to the high reactivity of the catalysts. The octahedral geometry of the Fischer-type carbene hinders the coordination of the alkene. The situation is only slightly changed by the dissociation of a CO ligand leading to the square-based pyramidal geometry of the catalyst. This molecular geometry is similar to the geometry of the Grubbs-type precatalyst before ligand dissociation necessary for metathesis reactivity. The Tebbe-type carbene has an essentially trigonal-planar geometry that should lead to easy alkene coordination. However, the cyclopentadienyl rings shield the metal atom almost completely.

Catalyst:	<i>Fischer_pre</i> (ML_6)	<i>Tebbe_pre</i> (ML_4)	<i>Grubbs_pre</i> (ML_5)	<i>Schrock</i> (ML_4)
	Octahedral	Tetrahedral	Square-based pyramidal	Tetrahedral
<u>Molecular geometry:</u>				
<u>Electron count^a:</u>	CO [L]: $= (5)(2) = 10$ C(Tol) ₂ [L]: $= (1)(2) = 2$ W: 6 Total $= 18$ electrons	η^5 -C ₅ H ₅ (Cp ₂) [L ₂ X]: $= (2)(5) = 10$ CH ₂ [X]: $= (1)(1) = 1$ Cl [X]: $= (1)(1) = 1$ Ti: 4 Total $= 16$ electrons	C(Ph) [L]: $= (1)(2) = 2$ PCy ₃ [L]: $= (1)(2) = 2$ NHC [L] ^b : $= (1)(2) = 2$ Cl [X]: $= (2)(1) = 2$ Ru: 8 Total $= 16$ electrons ^c	NAr [X ₂]: $= (1)(2) + 2$ (lone pair on nitrogen) ^d = 4 OR [X]: $= (2)(1) = 2$ C(R) [X ₂]: $= (1)(2) = 2$ Mo: 6 Total $= 14$ electrons
<u>Oxidation state:</u>	W(0)	Ti(IV)	Ru(II) ^c	Mo(VI)
<u>dⁿ Configuration of metal^a:</u>	d ⁶	d ⁰	d ⁶	d ⁰
<u>Electronic structure of the d block^a:</u>				

^a As acquired from [23], ^b as acquired from [1], ^c as acquired from [36] and ^d as acquired from [37].

Fig. 8. Theoretical treatment of the four main types of metal carbene precatalysts.

Catalyst:	<i>Fischer_cat</i> (ML_3)	<i>Tebbe_cat</i> (ML_3)	<i>Grubbs_cat</i> (ML_4)	<i>Schrock</i> (ML_4)
	Square-based pyramidal	Trigonal-planar	Tetrahedral	Tetrahedral
<u>Molecular geometry:</u>				
<u>Electron count^a:</u>	CO [L]: = (4)(2) = 8 C(Tol) ₂ [L]: = (1)(2) = 2 W: 6 Total = 16 electrons	η^5 -C ₅ H ₅ (Cp ₂) [L ₂ X]: = (2)(5) = 10 CH ₂ [X]: = (1)(1) = 1 Ti: 4 Total = 15 electrons	C(Ph) [L]: = (1)(2) = 2 NHC [L] ^b : = (1)(2) = 2 Cl [X]: = (2)(1) = 2 Ru: 8 Total = 14 electrons ^c	NAr [X ₂]: = (1)(2) + 2 (lone pair on nitrogen) ^d = 4 OR [X]: = (2)(1) = 2 C(R) [X ₂]: = (1)(2) = 2 Mo: 6 Total = 14 electrons
<u>Oxidation state:</u>	W(0)	Ti(III)	Ru(II) ^c	Mo(VI)
<u>dⁿ Configuration of metal^a:</u>	d ⁶	d ¹	d ⁶	d ⁰
<u>Electronic structure of the d block^a:</u>	b_1 $\overline{d_{x^2-y^2}}$ a_1 $\overline{d_{z^2}}$ b_2, e $\overline{d_{xy}}$ $\overline{d_{xz}}$ $\overline{d_{yz}}$	σ_g $\overline{d_{z^2}}$ π_g, δ_g $\overline{d_{x^2-y^2}}$ $\overline{d_{yz}}$ $\overline{d_{xz}}$ $\overline{d_{xy}}$	t_2 $\overline{d_{x^2-y^2}}$ $\overline{d_{yz}}$ $\overline{d_{xz}}$ e $\overline{d_{xy}}$ $\overline{d_{z^2}}$	t_{2g} $\overline{d_{x^2-y^2}}$ $\overline{d_{yz}}$ $\overline{d_{xz}}$ e_g $\overline{d_{xy}}$ $\overline{d_{z^2}}$

^a As acquired from [23], ^b as acquired from [1], ^c as acquired from [36] and ^d as acquired from [37].

Fig. 9. Theoretical treatment of the four main types of metal carbene catalysts.

6. Computational investigations of alkene metathesis

6.1 Fischer-type metal carbene catalysts

The metathesis reaction catalyzed by a W(0) complex, a pentacarbonyltungsten carbene, was studied by Tlenkopatchev and Fomine [38]. The reaction was modelled by using density functional theory (DFT) and second-order Moller-Plesset theory. In order for the olefin to be able to coordinate to the metal carbene one CO molecule must be eliminated to generate a vacant co-ordination site. This dissociation-complexation process was found to be thermodynamically controlled. Initiation of the carbene seems to be the rate-determining step followed by the dissociation of the olefin-catalyst complex. The metathesis reaction itself proved to have a very low activation energy. The calculated electronic factors support the theory that the LUMO has the largest coefficient at the carbene carbon and the HOMO has the maximum coefficient at the metal. Overlap between the olefin and the catalyst occurs between the HOMO of the olefin and the LUMO of the metallocarbene. The interaction between the olefin and the metal was also found to be due to the back donation from the d_{xy} orbital of the metal to the LUMO of the alkene. The highest orbital able to overlap with the LUMO of the alkene to form the olefin-metal bond was the HOMO-2 orbital of the molecule [38].

6.2 Tebbe-type metal carbene catalysts

A theoretical analysis of olefin metathesis, with $\text{Cp}_2\text{Ti}(\text{CH}_2)(\text{C}_2\text{H}_4)$ (Fig. 10) as model complex was done by Eisenstein and Hoffman [39].

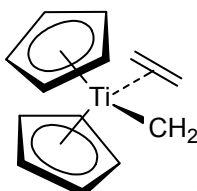


Fig. 10. $\text{Cp}_2\text{Ti}(\text{CH}_2)(\text{C}_2\text{H}_4)$ [39].

They found that only some orientations of the olefin relative to the carbene, as shown in Fig. 10, will be productive in metathesis. If the right conformations are obtained the catalysis is essentially done. Furthermore, the stable metal-carbene-olefin complex for many electron counts was found to be an intermediate non-classical structure (Fig. 11) rather than the metallacyclobutane.



Fig. 11. The intermediate non-classical structure of the metal-carbene-olefin complex [39].

The role of the metal was said to be in a sense merely the glue that holds the reactive partners, methylene and ethylene, in proximity. For the complex to form in the required orientation of olefin to carbene, the orbitals must be in the “collinear” conformation (Fig. 12). Calculations showed that the more positively charged metal will require a lower activation energy to reach the “collinear” geometry. [39]

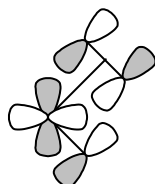


Fig. 12. The “collinear” orbital conformation [39].

Another study on Tebbe-type metal carbenes has been done by Upton and Rappé [40]. In their model they substituted the cyclopentadienyl rings with chloride. Previously it was found [41] that the chloride system seems to be a reasonable structural and energetic model of the dicyclopentadienyltitanacyclobutane. A common function of the chloro and cyclopentadienyl ligands was found to be the “removal” of 4s electron density from the Ti atom and to allow the formation of shorter bonds to the remaining 3d orbitals [40]. The absence of filled d-orbitals in this complex prevents back donation from the metal to the olefin leading to shorter C-C olefin bond distances

(1.34 Å). A mechanistic study on the Tebbe-type catalyst was also done by Axe and Andzelm [42]. They did DFT calculations and found the theory capable of describing interactions that govern structure and relative stability. However, it failed to describe the reactions [42].

6.3 Grubbs-type metal carbene catalysts

Most of the computational studies done on alkene metathesis focus on Grubbs-type metal carbenes. Together with Schrock-type metal carbenes they are the most active catalysts, however because the Grubbs-type catalysts are more air stable and easier to work with than the Schrock-type catalysts they are used more abundantly. Hence, a range of modeling studies has been done with Grubbs-type metal carbene catalysts. Adlhart and Chen [13] found that the difference between the activity of the first and second generation Grubbs catalysts is ligand rotation. This difference is brought about by a difference in symmetry of the ligands. The phosphine ligand has threefold symmetry. The need of phosphine to rotate causes a high barrier in the middle of the reaction coordinate. However, for the second generation Grubbs catalyst, with twofold symmetry of the NHC ligand, the barrier is absent [13]. The rate-limiting step for second-generation catalysts is always phosphine dissociation [13].

Another modeling study was done by Vyboishchikov, Bühl and Thiel [43]. They did DFT calculations on the mechanism of the metathesis reaction of ethene and model catalysts $[(\text{PH}_3)(\text{L})\text{Cl}_2\text{Ru}=\text{CH}_2]$ with $\text{L}=\text{PH}_3$ and $\text{L}=\text{C}_3\text{N}_2\text{H}_4 = \text{imidazole-2-ylidene}$. Both the associative and the dissociative mechanistic pathways were calculated. For the associative pathway the rate-determining step for both catalysts was the initial olefin coordination. In the dissociative pathway the incoming olefin can coordinate to the active catalyst either *cis* or *trans* to the ancillary ligand L [43]. Because *cis* ethene attack requires a large activation energy, the dissociative mechanism with *trans* olefin coordination is preferred. The *trans*-coordination is electronically allowed because of the possibility of frontier orbital overlap between the catalyst and ethene. The LUMO of the catalyst, predominantly the $d_{x^2-y^2}$ of the Ru atom, is oriented for π donation of the HOMO of ethene to the LUMO. The HOMO of the catalyst is also oriented for

back donation to the π^* of ethene [43]. The rate-determining step in the dissociative pathway was thus calculated to be the rearrangement of the *trans*-adduct and the ruthenacyclobutane. The dissociative mechanism was found to be favored above the associative mechanism. This result is also supported by the study of Fomine, Vargas and Tlenkopatchev [44] who calculated the metathesis reactions of propylene with model catalysts $\text{Cl}_2(\text{PMe}_3)_2\text{Ru}=\text{CH}_2$ and $\text{Cl}_2(\text{PCy}_3)_2\text{Ru}=\text{CH}_2$. Another paper with model catalysts and ethylene show similar results [45].

Cavallo [46] performed a DFT study of the Ru-catalyzed metathesis reaction of ethene. He found that the NHC-based catalyst has a higher propensity to bind to the ethene than the dissociated phosphine ligand, increasing the activity. The higher activity of the NHC-based catalyst can also be explained by the lower metathesis insertion barrier than that of the first generation Grubbs catalysts. Results showed that the metallacyclobutane structures are local minima along the reaction coordinate. Furthermore, the NHC-based catalyst promotes olefin coordination and stabilizes the metallacycle intermediate, enhancing the overall activity [46].

Costabile and Cavallo [47] investigated the origin of enantioselectivity in the asymmetric Ru-catalyzed metathesis. Janse van Rensburg *et al.* [48] predicted the substrate-induced catalyst decomposition in ruthenium-catalyzed metathesis with DFT. The understanding of catalyst decomposition pathways would lead to increased catalyst efficiency. They proposed decomposition involving β -hydride transfer from a ruthenacyclobutane intermediate [48].

Another modeling study done by Adlhart and Chen [49] focused on using different substrates to model the four classes of olefin metathesis: acyclic degenerate, acyclic exothermic, and ROMP with either an unstrained or a strained cyclic olefin on the complete system. They also found the *trans*-dissociative pathway to be the most favourable supporting the results of Vyboishchikov, Bühl and Thiel [43]. The rate-limiting step was again proved to be the dissociation of the phosphine ligand as was found in one of their previous studies [13].

Suresh and Koga [50] conducted a study on the alkene metathesis of ethene with the model bisphosphine complex $(\text{PH}_3)_2\text{Ru}(\text{CH}_2)\text{Cl}_2$. According to them the first transition state for the formation of the metallacyclobutane intermediate is the rate-determining step of the metathesis reaction. They attributed the low barrier of the rate-determining step to two main orbital interactions (a) the strong π -orbital interactions between the $\text{Ru}=\text{CH}_2$ and the alkene moiety in the transition state and (b) the two agostic orbital interactions in the metallacyclobutane [50]. A quantum molecular dynamics study by Aagaard, Meier and Buda [51] done on the same system supports the generally accepted alkene metathesis mechanism and the need for carbene rotation. According to Straub [52] the origin of the high activity of second-generation Grubbs catalysts is the electronic and steric stabilization of the active conformation of the carbene moiety by the NHC σ -donor ligand (Fig. 13).

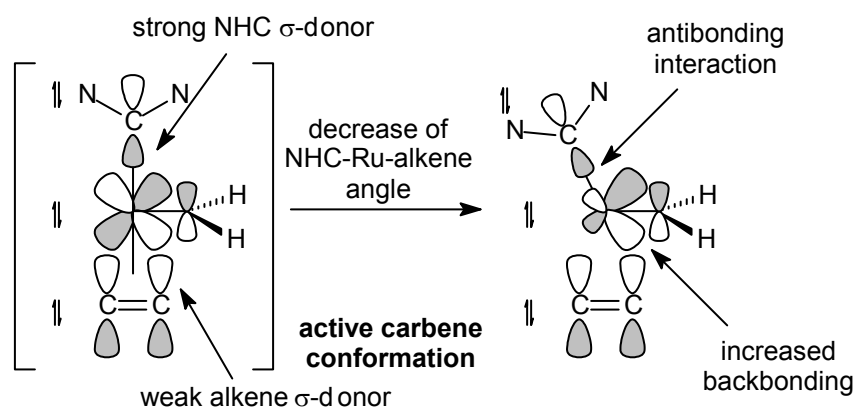


Fig. 13. Stabilization of active carbene orientations [52].

A DFT study on the stereochemistry of ring-closing olefin metathesis by second-generation ruthenium-containing Grubbs catalysts was done by Vyboishchikov and Thiel [53]. It was found that the stereochemistry of the cyclo-olefin product was determined either during the metallacycle formation or cleavage. However, by changing the catalyst or the substrate, the precise pathway can be changed but the overall reaction mechanism remains unaltered [53].

Tsipis, Orpen and Harvey [54] studied the substituent effects by exploring the potential energy surfaces of the metathesis reaction using a hierarchy of models,

ranging from $[(L)(\text{PH}_3)\text{Ru}(\text{Cl})_2(\text{CH}_2)]$ ($L = \text{PH}_3$ or diaminocarbene) through the larger $[(L)(\text{PMe}_3)\text{Ru}(\text{Cl})_2(\text{CHPh})]$ to the “real” $[(L)(\text{PCy}_3)\text{Ru}(\text{Cl})_2(\text{CHPh})]$. They found the rate-limiting steps after phosphine dissociation to be the transition states leading to the ruthenacycle intermediate. The fast reaction rate after phosphine dissociation is attributed to the transition states being very close in energy to the 14 electron active catalysts. Again the higher activity of the second-generation catalysts is credited to the greater electron-donating strength of the NHC-ligand [54].

In a study done by Correa and Cavallo [55] on the mechanism catalyzed by a (NHC)Ru-based catalyst, they concluded that it is a trade-off between steric, electronic and solvent effects. In most of the five cases studied by Correa and Cavallo, for the reaction of ethylene with the model complex, they found that the bottom-bound intermediate pathway is favored as opposed to side-bound intermediate pathway (Fig. 14). In the bottom pathway the alkene bonds trans to the NHC ligand.

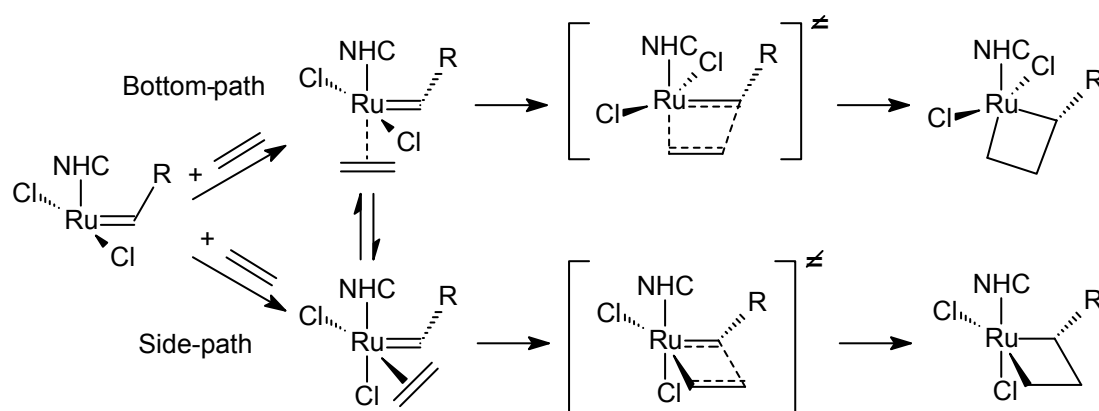


Fig. 14. Postulated substrate binding *cis* (side path) or *trans* (bottom path) to the NHC ligand [55].

Benitez, Tkatchouk and Goddard III [56] investigated the relevance of *cis*- and *trans*-dichloride in Grubbs-II metathesis catalysis to effect diastereo- and enantioselectivity. They found conclusively that the mechanism pathway is bottom-bound, as proposed by Correa and Cavallo [55] (Fig 14.), and the chlorides remain *trans* throughout the reaction.

Occhipinti, Bjørsvik and Jensen [57] did a quantitative structure-activity relationship (QSAR) study of ruthenium catalysts with DFT. They used model 14-electron complexes, $\text{LCl}_2\text{Ru}=\text{CH}_2$, with 82 different dative ligands, L, and ethylene as olefin. The proposal is that knowledge of the relationship between the nature of the ligand L and the resulting activity is essential for further catalyst development [57]. Two main effects were considered, namely: electronic effects and steric effects. Table 2 [57] shows the molecular descriptors for the final QSAR model and their respective contributions to the productivity, as defined in Fig. 15, of the catalysts.

Table 2 Molecular descriptors and their regression coefficients (β) in the QSAR model [57]

molecular descriptor	β
Wiberg index for the Ru=CH ₂ bond	1.389
Ru=CH ₂ σ bond order	1.101
steric exchange repulsion L-alkylidene	0.976
total dipole of the molecule (CHELPG)	0.900
L→Ru σ -donation	0.757
average electrophilic reactivity index for a C atom	0.650
relative number of single bonds	0.620
1-electron reactivity index for the Ru atom	0.453
ZX shadow/ZX rectangle	0.434
minimum nucleophilic reactivity index for a C atom	0.390
maximum bond order of a H atom	0.290
maximum valency of a C atom	0.237
HOMO-LUMO energy gap	0.131
Ru d_{π} →L $_{\pi}$ back donation	-0.290
moment of inertia B	-0.409
average nucleophilic reactivity index for a C atom	-0.536
total hybridization comp. of molecular dipole	-0.619
relative negative charge (RNCG)	-0.627
electrophilic reactivity index for the Ru atom	-0.686
maximum bond order of a C atom	-0.730
Kier and Hall index (order 2)	-0.985
Ru=CH ₂ bond distance	-1.419

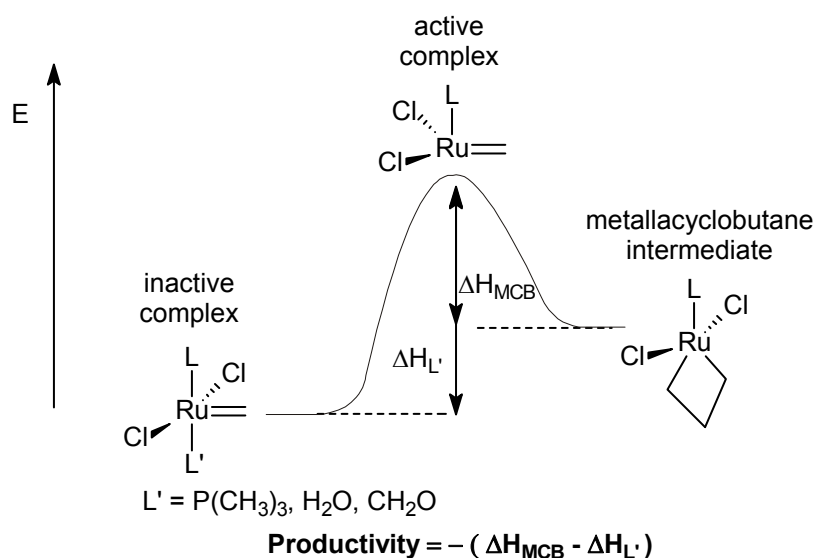


Fig. 15. Definition of “productivity” as used as the response variable in the QSAR model building [57].

The two enthalpy differences in Fig. 15 are given with respect to the 14-electron active complex. $\Delta H_{L'}$ is thus always negative, and ΔH_{MCB} is found to be positive only for a few of the catalysts with very low calculated productivities [57]. The best positive productivity correlation for the electronic effect is achieved by the Wiberg bond order index [58] for the Ru=CH₂ bond. However, the corresponding bond distance was calculated to be negatively correlated. These results enforce the importance of a strong ruthenium-alkylidene bond. The catalysts with the highest productivity have Wiberg bond orders of well above 1.6 [57]. To determine the steric effect of the dative ligands, the steric exchange repulsion between the ligand, L, and the methylidene in the 14e⁻ complex was calculated. It turned out to be “strongly positively correlated with productivity” [57]. The difference between the Grubbs second generation and Grubbs first generation catalysts was concluded to be the specific steric pressure exerted by the NHC ligand on the alkylidene moiety. Thus, from the QSAR model, new possible metathesis catalysts could be predicted based on the selection of ligands. Accordingly, carbenes described by Arduengo were found to possess the predicted steric and electronic properties for possible olefin metathesis

catalysis. Furthermore, for NHC ligands, the nitrogen atoms should bear large and σ -donating substituents [57].

In a further study Janse van Rensburg *et al.* [59] investigated the relative reactivity and decomposition behaviour of three ruthenium catalysts: first and second-generation Grubbs catalysts and the Phoban catalyst (“Phobcat”). The Gibbs free energy surface at 298.15K and 1 atm was calculated for each catalyst. No simplification model was used for the catalysts [59]. The catalyst initiation, ethylene coordination and ruthenacyclobutane formation as well as the ruthenacyclobutane decomposition were studied. For the ethylene coordination step they found that different ethylene/methylidene orientations form the lowest energy Ru-ethylene π -complexes of the three catalysts. Therefore, significant rotation of the methylidene and ethylene was found that formed part of the single imaginary normal modes for the transition state structures [59]. The substrate-induced ruthenacyclobutane decomposition was calculated to follow the increasing order: second-generation < Phobcat < first-generation [59].

Straub [60] did a DFT study on the ligand influence on the reactivity of ruthenium metal carbene catalysts. By understanding the effect of the ligands, new catalysts can be designed with greater activity. The success of the first and second-generation Grubbs catalysts can be ascribed to the σ -donating ability of the phosphine and NHC-ligand. According to the rule of Grubbs [61] the phosphine ligands and later the NHC-ligand, which are larger and more electron-donating, combined with the smaller and more-electron-withdrawing halogens, led to more active catalysts. The difference in activity between the active catalysts, after ligand dissociation, is due to electronic effects [53]. Thus, the rate of ruthenacyclobutane formation differs. Because of possible ligand rotation, the formation of active and inactive carbene conformations is proposed. Fig. 16 shows the difference in activity between the first and second-generation Grubbs catalysts, with ligand rotation barriers in the order of 10 kJ mol⁻¹ [60]. The main origin of the higher activity of the second-generation Grubbs catalyst lies in the electronic stabilization of the active carbene conformations.

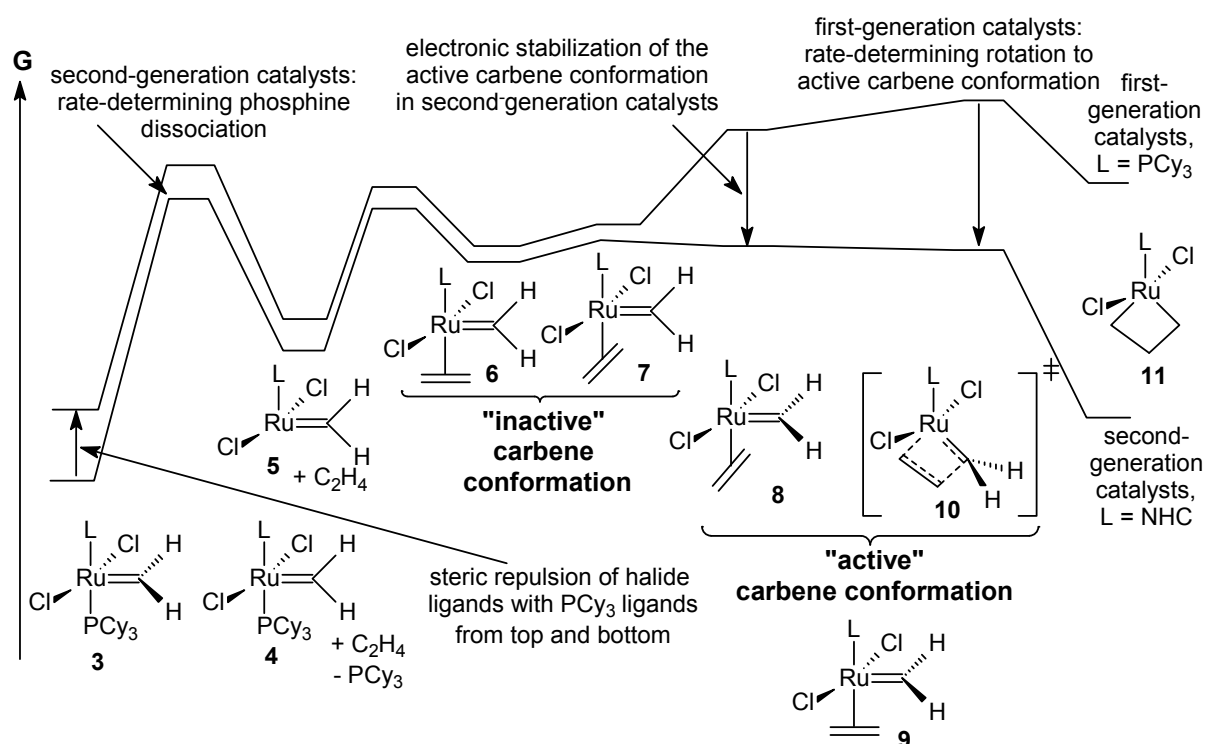


Fig. 16. Gibbs free energy profile of the mechanism of first- and second-generation Grubbs catalysts. The carbene rotation barriers are in the order of 10kJ mol^{-1} [60].

Therefore, the effect of the anionic ligands on the reaction pathway was evaluated. Different ligands, as well as *cis* and *trans* conformation of the anionic ligands, were computed. By varying the halogens the catalytic activity was found to be $\text{Cl}_2(\text{L})\text{Ru}=\text{CH}_2 > \text{Br}_2(\text{L})\text{Ru}=\text{CH}_2 \gg \text{I}_2(\text{L})\text{Ru}=\text{CH}_2 \gg \text{F}_2(\text{L})\text{Ru}=\text{CH}_2$. Alkoxide and thiolate ligands were also found to be less superior than chloride. Three factors were named that are thus mandatory to catalyst activity: the fast and facile formation of the 14 valence electron species; strong σ donors *trans* to the alkene and poor σ donor ligands *cis* to the alkene ligand; and the ligand sphere has to be inert towards the electrophilic carbene moiety [60]. Subsequent to this study was a study of Naumov and Buchmeiser [62] that implements the same mechanism and reasoning as Straub [53],[60] to investigate the ROMP of norborn-2-ene.

According to an experimental proposal by Romero and Piers [63] on the degenerate ethylene exchange (Fig. 17), Webster [64] followed up with computational insights.

Inter- and intramolecular exchange of ethylene in the ruthenacyclobutane intermediate were studied. Support was provided for the single step-intramolecular mechanism and for an associative multistep intermolecular mechanism for the exchange of ethylene [64].

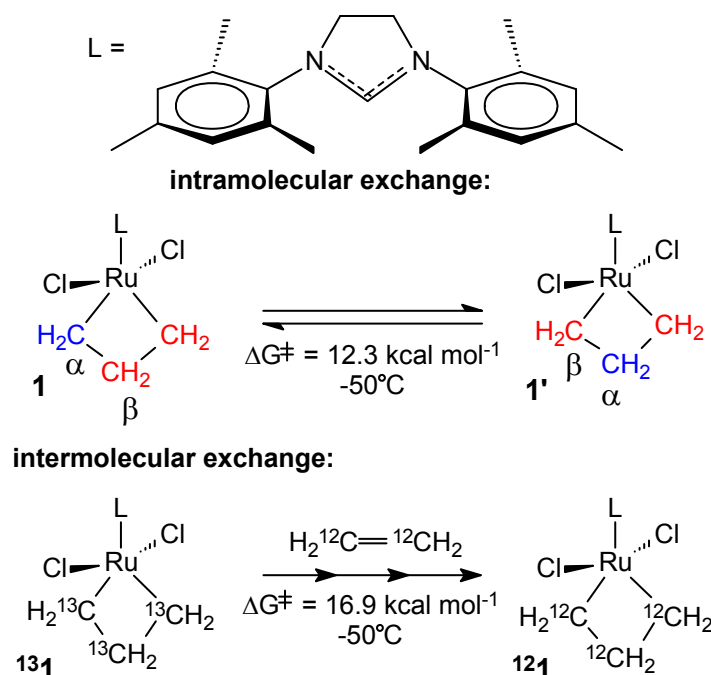


Fig. 17. Experimental observations by Romero and Piers [64].

Getty, Delgado-Jaime and Kennepohl [65] tried to rationalize the observed initiation rates of ruthenium catalyzed metathesis by investigating the charge donation in phosphine and NHC ligands. The charge on the metal atom is more positive for the NHC-bound complex than for the bisphosphine complex [65]. The decrease in electron density at the metal atom can be explained by the increase in π -back bonding to the NHC ligand. This is also proposed as the reason for slower phosphine dissociation of the second-generation Grubbs catalysts [65].

Poater *et al.* [66] explored the reactivity of Ru-based catalysts with the coordination of a CO molecule *trans* to the Ru-ylidene bond. The coordination of the CO leads to greater “free-carbene” character of the methylidene and finally to the deactivation of the catalyst.

Weskamp *et al.* [67] did a DFT study on the NHC ruthenium carbene catalysts. They showed that combining the NHCs with coordinatively more labile ligands on the ruthenium atom, as is the case for the second-generation Grubbs catalysts, allows the NHCs to be most effective as ligand [67]. Because phosphine dissociation is the key step for catalyst initiation, they calculated the dissociation energies of NHC and phosphines for the ruthenium carbene model compounds shown in Fig. 18.

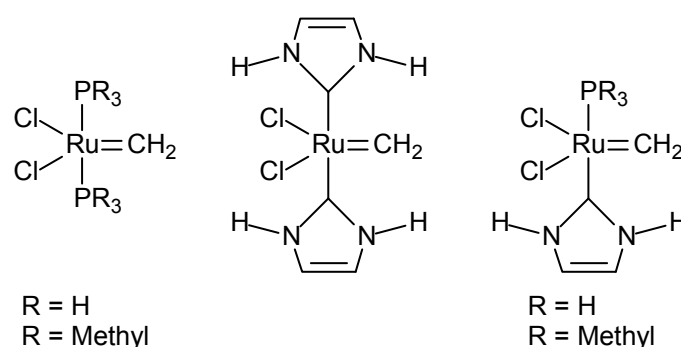


Fig. 18. Model compounds for calculation of ligand dissociation energies [67].

The results show that dissociation energy increases from $\text{PH}_3 < \text{PMe}_3 < \text{NHC}$ thus revealing the advantage of a mixed NHC/phosphine complex [67].

Meier, Aagaard and Buda [68] did a molecular dynamics study on the ethylene metathesis reaction with the first-generation Grubbs-type model catalysts. They proved by simulation studies the need for phosphine dissociation to activate the catalyst. Furthermore, it was shown that the higher metathesis activity of sterically crowded phosphines can be rationalized by their intrinsically more labile Ru-P bonds [68].

In a study done by Jacobsen [69], the nitrogen in the NHC ligand was substituted with phosphorus to form PHC carbene catalysts. Metathesis reactions involving ethene and several model catalysts of the type $(\text{PR}_3)(\text{EHC})\text{Cl}_2\text{Ru}=\text{CH}_2$, $R = \text{H}, \text{CH}_3$, and $E = \text{P}, \text{N}$ were investigated (Fig. 19).

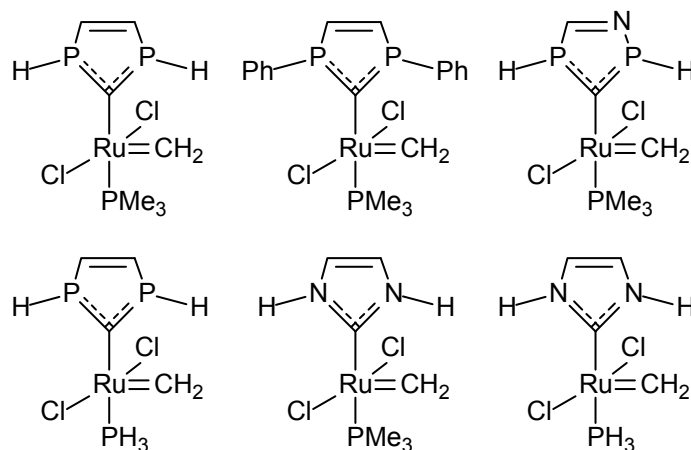


Fig. 19. Model NHC and PHC catalysts studied by Jacobsen [69].

The results show that, similar to the NHC-type catalysts, the PHC-type catalysts also follow the dissociative reaction pathway. Whereas the rate-limiting step for the NHC-type catalysts is phosphine dissociation, the rate-limiting step for the PHC-type catalysts is the ring-opening of the ruthenacyclobutane intermediate. Although the initiation step (phosphine dissociation) is lower for PHC-type catalysts, NHC ligands promote olefin coordination more effectively than PHC ligands, leading to more active metathesis catalysts. A similar study on PHC ligands versus the NHC ligands has also been done by Schoeller, Schroeder and Rozhenko [70].

A study done by Jordaan *et al.* [16], on the metathesis reaction of 1-octene with the first generation Grubbs catalysts, shows the need of considering the complete catalyst and reagent molecules as well as the complete catalytic system for computation of the reaction. The real systems are shown to be much more complex, with electronic and steric effects playing a large role in the activity of the systems. True conclusions cannot be made when only considering simple systems [16]. This result is also supported by Marx, Jordaan and Vosloo [19] who did a study on the complete catalytic cycle of the 1-octene metathesis reaction mechanism with the Phobcat precatalyst.

Lord *et al.* [71] did a DFT study on the second generation Grubbs catalyst. They investigated the molecular orbital diagram and the structure-reactivity relationship of

saturated and unsaturated NHC ligands. Specifically the metallacyclobutane structure was calculated. Fig. 20 [71] shows the simplified MO-diagram of the four model metallacyclobutane structures calculated. Various bonding options with the metallacyclobutane because of possible ligand rotation are displayed. Instead of the expected π^* -system metal-ligand bonding interactions, interactions are only observed with the π -system [71].

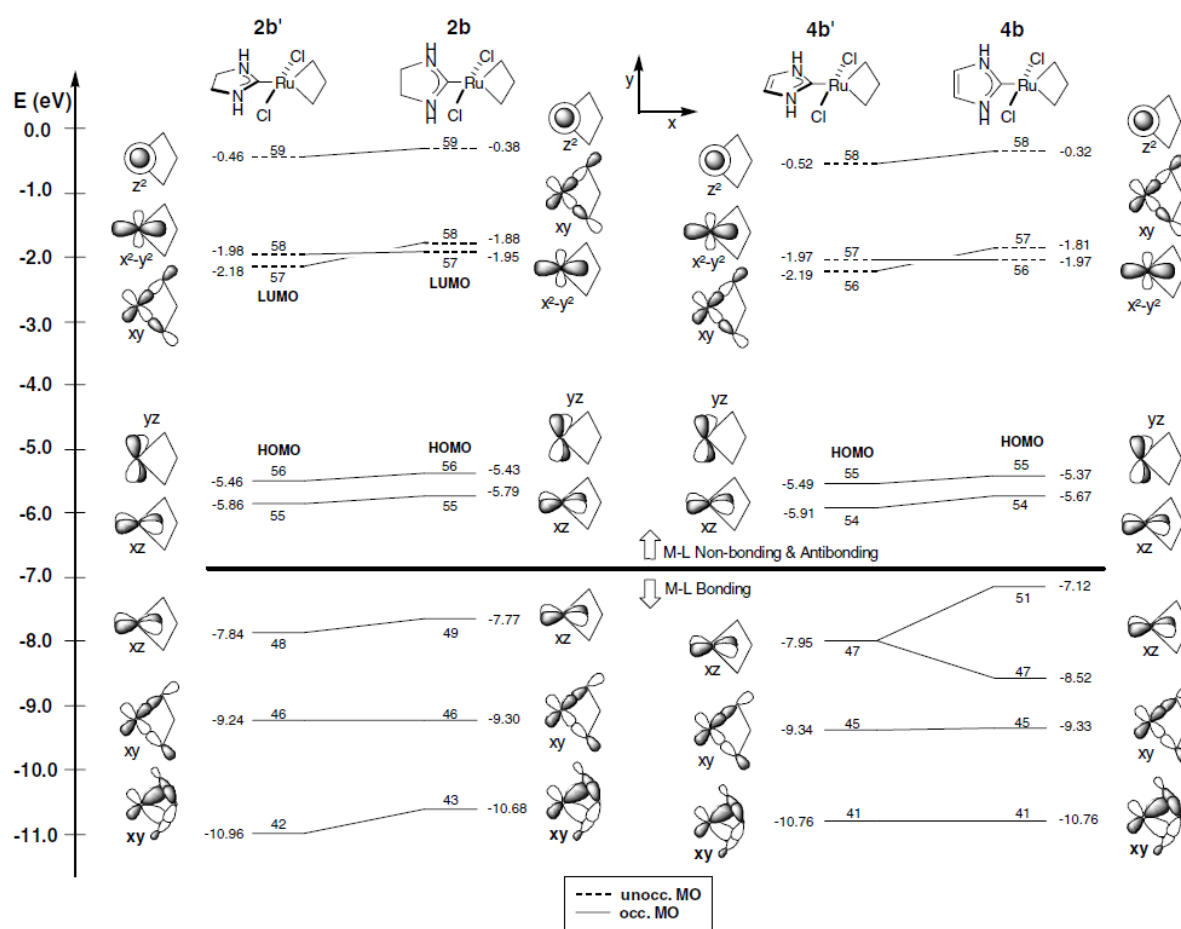


Fig. 20. MO-diagram comparing the most important molecular orbitals of the four models [71]. (Reproduced with permission, copyright (2006) Elsevier.)

Fernández, Lugan and Lavigne [72] investigated the effect of π - π^* attractive interactions through space in the second generation Grubbs catalyst. They specifically investigated the short distance between the C_{ipso} (N -aryl) and the $C_{alkylidene}$ carbon atoms (Fig. 21) for a possible stabilizing interaction between the respective molecular orbitals [72]. By using the second-order perturbation theory of the natural bond orbital

(NBO) method [73], they found an occurrence of a stabilizing interaction (Fig. 22). The reason for the stabilizing interaction to be a plausible option for the enhanced activity, above the previously believed π -stacking interaction, is that it can remain operative through the whole catalytic cycle [72].

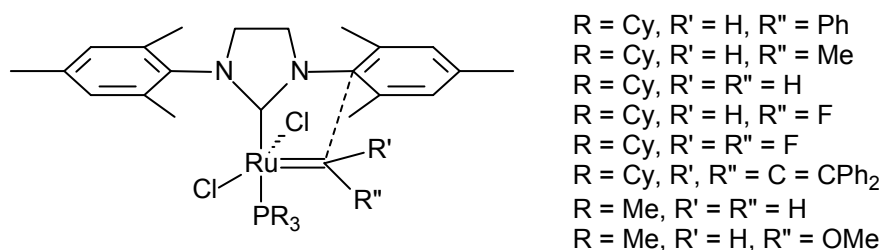


Fig. 21. Second generation Grubbs-type catalysts studied by Fernández, Lugan and Lavigne [72].

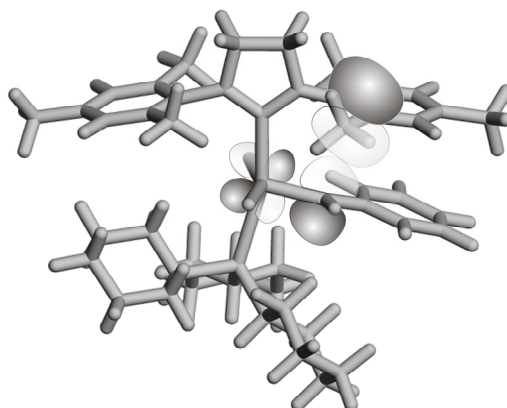


Fig. 22. NBO-molecular orbital interaction that stabilizes the complex [72].

Recently a few studies have been done on the Hoveyda-Grubbs second generation precatalysts, including the study done by Van der Gryp, Marx and Vosloo [74]. They investigated the dissociative mechanistic pathway of the 1-octene catalyzed metathesis reaction. Experimental work, done in coordination with the DFT calculations, were validated by the results of mechanistic investigation. According to Nuñez-Zarur *et al.* [75] the activation step plays an important role in the overall reactivity of these catalysts. Consequently, they studied the electronic structure of 15 different Hoveyda-Grubbs precatalysts by means of DFT [75]. Another study was also done by Nuñez-

Zarur *et al.* [76] where the differences in activation processes of phosphine-containing and Hoveyda-type catalysts were compared. Ashworth *et al.* [77] identified the initiation step in the Grubbs-Hoveyda precatalyst as the rate-limiting step. Furthermore, the initiation step was found to be an interchange rather than a dissociative step.

Various other studies have been done on specific ruthenium catalyzed olefin metathesis reactions [78-88] as well as on specific ruthenium containing catalytic systems [89-97].

6.4 Schrock-type metal carbene catalysts

Goumans, Ehlers and Lammertsma [98] did a computational study on the asymmetric Schrock olefin metathesis catalyst. An initial reaction with ethylene and a simplified model Schrock catalyst $(\text{MeO})_2\text{Mo}(\text{CH}_2)\text{NH}$ was calculated to establish the general mechanism outline (Fig. 23). The calculations were then repeated with the complete reaction (Fig. 24).

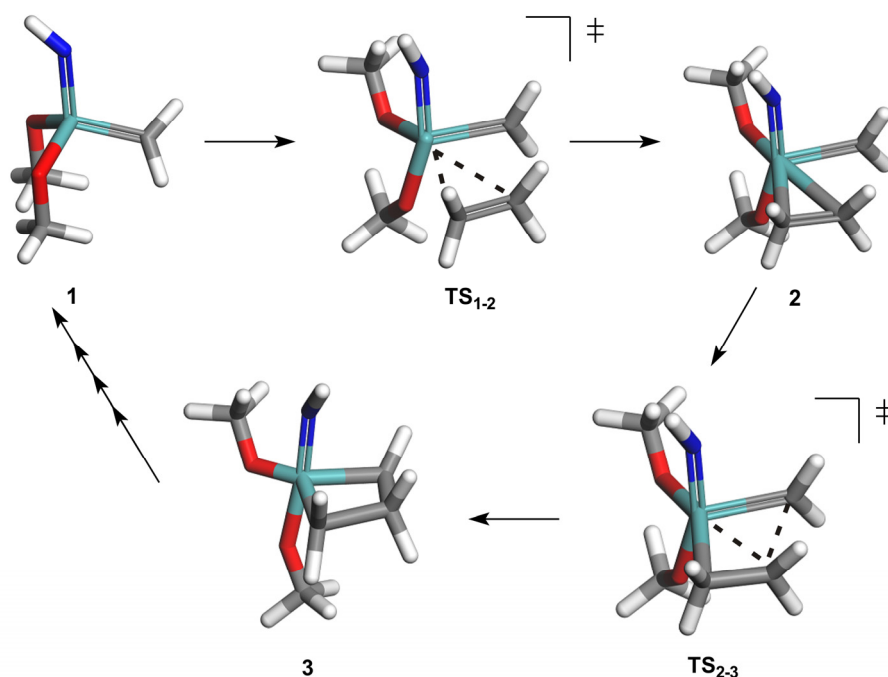


Fig. 23. Calculated structures of the mechanism of ethylene and the simplified Schrock catalyst [98].

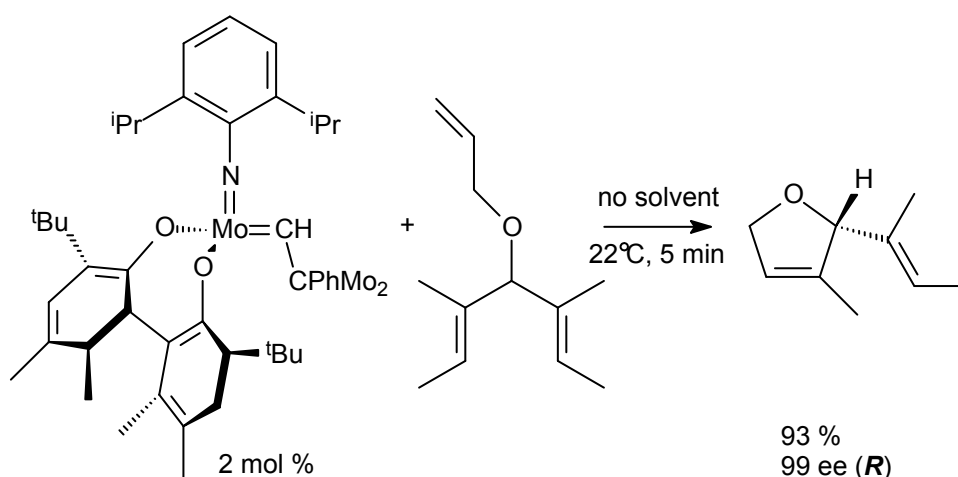


Fig. 24. Catalytic desymmetrization of a prochiral triolefin [98].

Due to the complexity of the system and the extreme demand on the computer resources transition states for the reaction could not be found. However, the enantioselectivity of the system could be reproduced computationally [98].

A comparative study was done by Poater *et al.* [99] on the Schrock-type carbene framework by respectively changing the metal and spectator ligands (Fig. 25).

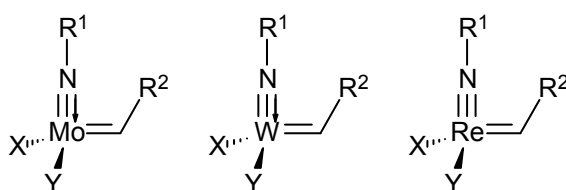


Fig. 25. d^0 Schrock-type carbene framework [99].

The idea is that a catalyst, with an electropositive metal and an X and Y pair of electronegative alkoxy ligands, is more efficient [99]. The ethene metathesis reaction with model catalysts where $R^1 = \text{CH}_3$ or Ph and $X = Y = \text{OCH}_3$, CH_2CH_3 or OSiH_3 was calculated. Only the attack of ethene from the back or the front of the catalysts has been studied. Two factors were found that influence the activity of the catalysts, namely: the ability of the catalyst to distort to open a coordination site for the incoming olefin, and the stability of the metallacyclobutane. It was proposed that

catalysts with different X and Y ligands are more effective, with one being a good donor ligand (alkyl) and one a poor σ -donor ligand (alkoxy and siloxy) [99]. A similar study was previously done by Solans-Monfort *et al.* [100] only on the Re-based catalysts.

Vasiliu *et al.* [101] calculated the bond energies in model Schrock metathesis catalysts. To understand better the energetics underlying their catalytic behavior, they calculated the bond dissociation energies (BDEs) and the heats of formation of the compounds (Fig. 26). The role of the electronegativity on the carbene was also studied along with the initial complexation reaction with ethene [101].

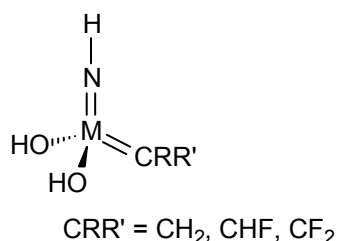


Fig. 26. The model Schrock compounds with M = Cr, Mo and W [101].

The results show the order of BDEs for the model complex to be $M=N(H) > M-O(H) > M=CRR'$, except in the case of $Mo=CH_2$ which is just larger than $Mo-O(H)$. Furthermore, it was shown that carbene centers involved in metathesis reactions need to have triplet ground states to form good $M=C$ bonds [101]. The model compounds were also predicted to be weak Brønsted acids and modest Lewis acids making it possible to design a catalyst soluble in aqueous solution [101].

Cundari and Gordon [102] investigated model Schrock carbenes (Fig. 27) for the effect on bonding caused by modification of either the metal, ligands or alkylidene substituents.

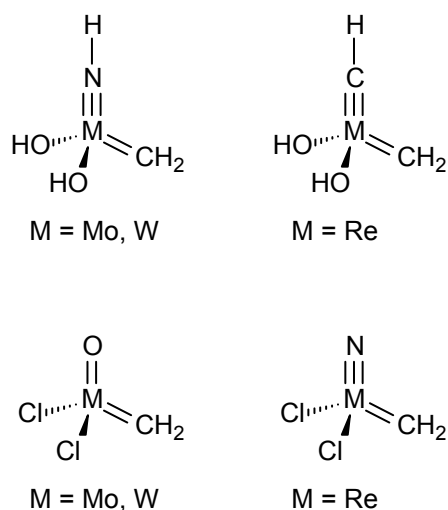


Fig. 27. Model Schrock-type carbenes investigated by Cundari and Gordon [102].

Two main conclusions were reached. To reach the minimum energy structure maximum metal $d\pi$ to ligand $p\pi$ bonding is necessary. Because ligands compete for this $d\pi$ AO, the balance is upset when the alkylidene group is rotated about the MC bond axis. Reorganization of the ancillary ligands is then needed to maintain a maximum amount of MC π bonding. The barrier height is thus controlled by the ability of the ancillary ligand's distortion [102]. Furthermore, the MC bond polarity of $\text{W}(\text{OH}_2)(\text{NH})(\text{CH}_2)$ versus $\text{Mo}(\text{OH}_2)(\text{NH})(\text{CH}_2)$ correlates with metathesis activity. The more positive the metal, the more active the catalyst for metathesis [102].

Folga and Ziegler [103] did a DFT study on the molybdenacyclobutane and its role in metathesis. They studied the electronic and molecular structure of the model compound $(\text{L})_2\text{Mo}(\text{X})\text{CH}_2$ with $\text{L} = \text{Cl}, \text{OCH}_3$ and OCF_3 and $\text{X} = \text{O}$ and NH . The frontier orbitals of the free carbene, square-pyramidal (SP) and trigonal-bipyramidal (TBP) framework (Fig. 28) were calculated with $\text{L} = \text{CH}_3\text{O}$ and $\text{X} = \text{NH}$.

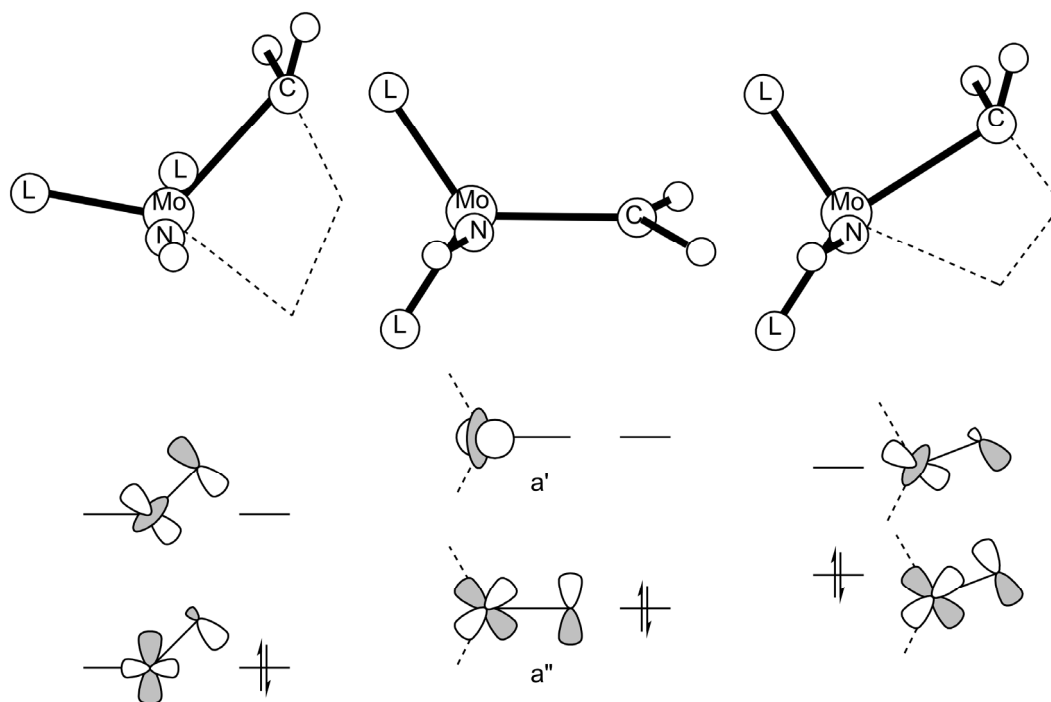


Fig. 28. Frontier orbitals of the model compound $(L)_2Mo(X)CH_2$ with $L = OCH_3$ and $X = NH$ [103].

By changing the ligand L to Cl or OCF_3 the two frontier orbitals were stabilized. The electron-donating methoxy groups destabilize the frontier orbitals. Thus, the energy of the frontier orbitals in Fig. 28 is primarily affected by changing the L ligand [103]. No significant changes to the frontier orbitals were observed when changing the X ligand to O from NH . For the formation of the metallacycle the $L = Cl$ and ethene was used as alkene (Fig. 29) [103].

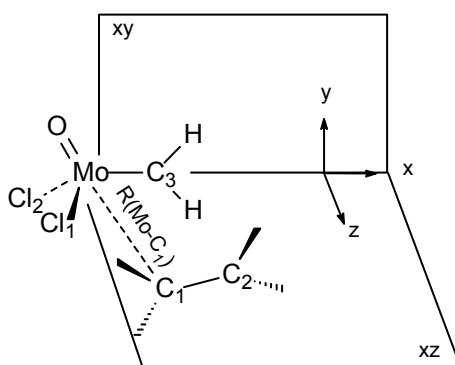


Fig. 29. The approach of ethene perpendicular to the $O-Mo-C_3$ (xy) plane of the metal carbene complex [103].

Formation of the metallacycle was calculated by shortening the R(Mo-C₁) distance stepwise. Because of symmetry considerations a correlation diagram of the possible overlaps for the formation of the metallacyclobutane is shown in Fig. 30 [103].

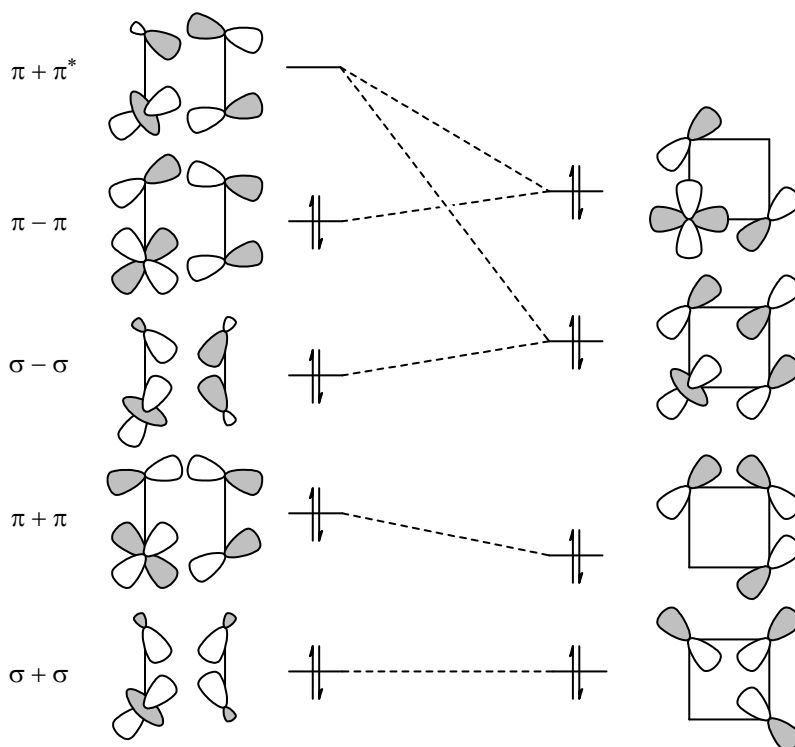


Fig. 30. Correlation diagram of the possible overlaps for the formation of the metallacyclobutane [103].

Two possible pathways were considered, namely: the formation of the SP or TBP metallacyclobutane frameworks (Fig. 31) [103].

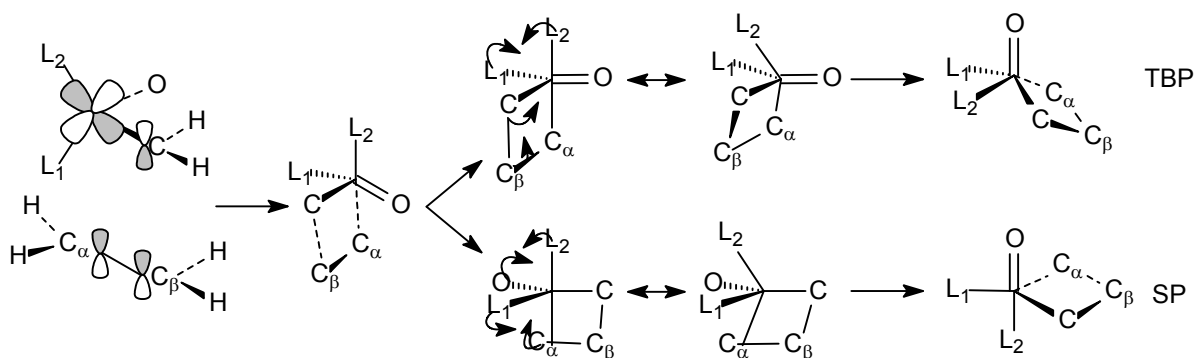


Fig. 31. The two possible pseudorotation pathways for formation of the SP and TBP metallacyclobutanes [103].

For the TBP pathway they propose a two-step attack for the formation of the metallacycle which includes an initial nucleophilic attack of the alkene C_1 carbon at the metal atom (Fig. 32) and the later nucleophilic attack of the carbene C_3 atom at the olefinic C_2 carbon (Fig. 33) [103]. They calculated that the concerted approach of the donor and acceptor interactions simultaneously would lead to C_2-C_3 and $M-C_1$ antibonding interactions (Fig. 34) [103].

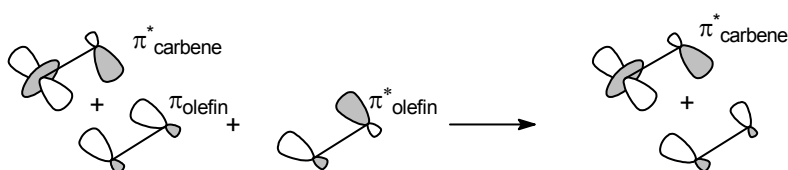


Fig. 32. Nucleophilic attack of the olefin C_1 carbon on the metal atom for the TBP pathway [103].

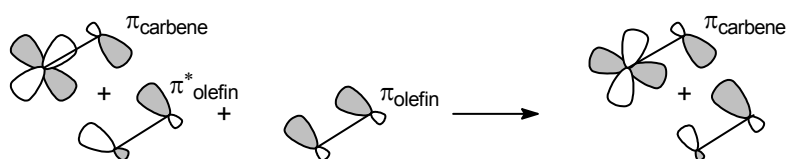


Fig. 33. Nucleophilic attack of the carbene C_3 atom at the olefinic C_2 carbon for the TBP pathway [103].

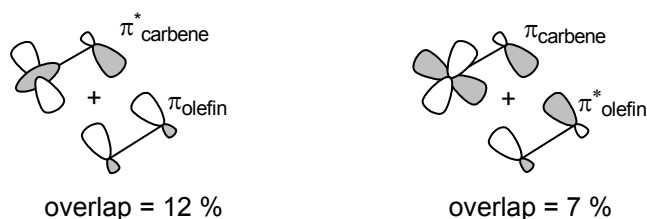


Fig. 34. Concerted C_2-C_3 and $M-C_1$ antibonding interactions for the TBP pathway [103].

The corresponding donor/acceptor orbitals of the SP pathway are shown in Fig. 35 [103]. Because of the change in geometry the interactions are more prone to a concerted approach.



Fig. 35. Concerted C₂-C₃ and M-C₁ antibonding interactions for the SP pathway [103].

The results showed that electron-withdrawing ligands (OCF₃) lead to the formation of the TBP intermediate, whereas the electron-donating ligands (OCH₃) lead to the formation of the SP intermediate [103].

Fox, Schofield and Schrock [104] also did a study on the electronic structure of Mo(VI) alkylidene complexes supporting the work of Folga and Ziegler [103]. They especially looked at the orbital evolution during alkylidene ligand rotation and an alternative method for metallacyclobutane formation via the rotation of the alkylidene ligand by 90°. The ground state valence molecular orbital energies of Mo(NH)(CH₂)(OH)₂ were calculated. Fig. 36 [104] shows the calculated Mo-N π-antibonding interaction (LUMO) in the *xz* plane of the complex after alkylidene ligand rotation of 90°. The orbital is essentially a non-bonding metal-centered d_{xy} orbital (72%) which has only minor contributions from each of the other bonding atoms [104]. The evolution of the orbitals during ligand rotation is shown in Fig. 37.

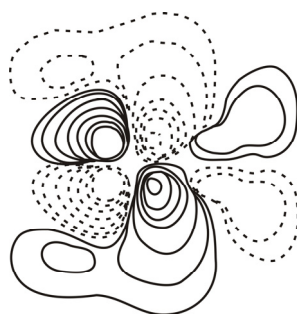


Fig. 36. The Mo-C π-antibonding interaction (LUMO) in the *xy* plane in Mo(NH)(CH₂)(OH)₂ with the alkylidene ligand rotated by 90° [104].

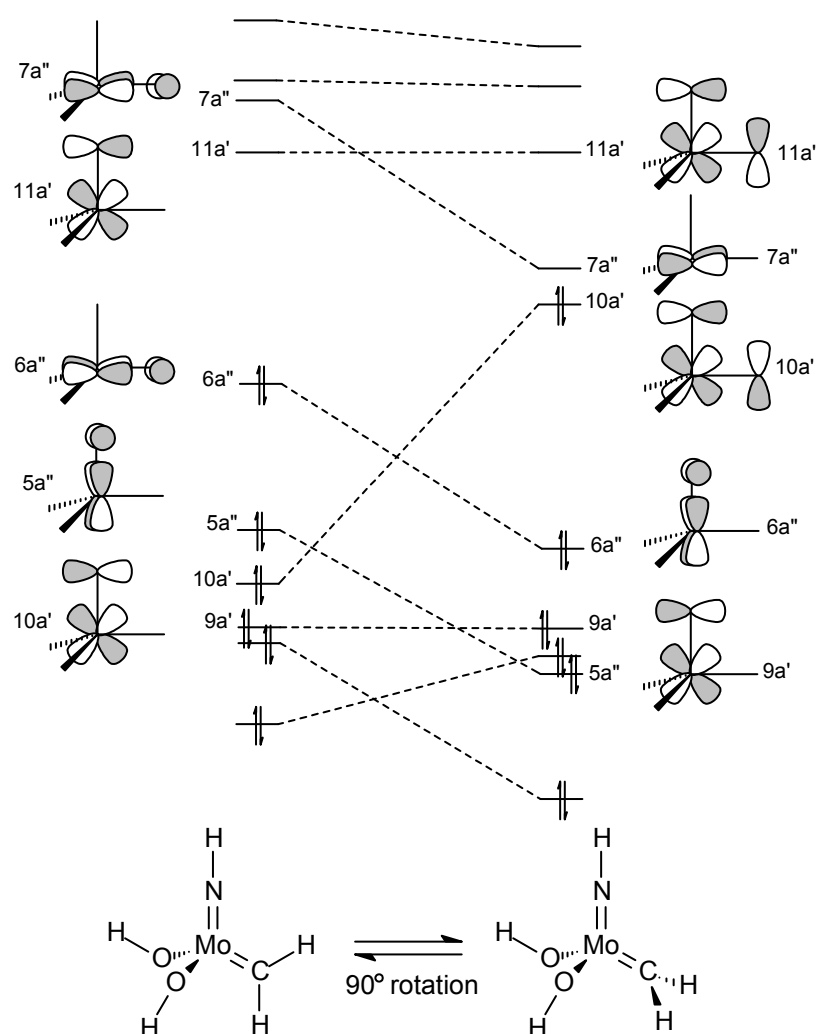


Fig. 37. Orbital evolution during alkylidene rotation depicting pertinent π molecular orbitals for (0°) and (90°) [104].

In the subsequent calculated metathesis reaction of ethene catalyzed by the model molybdenum catalyst, the π -bonding orbital (HOMO) of the alkene overlaps with the π -antibonding orbital (LUMO) of the rotated pseudotetrahedral alkylidene complex to form the metallacyclobutane (Fig. 38). The alkene attacks the COO face of the complex (Fig. 39) and not the CNO face as described by Folga and Ziegler [103].

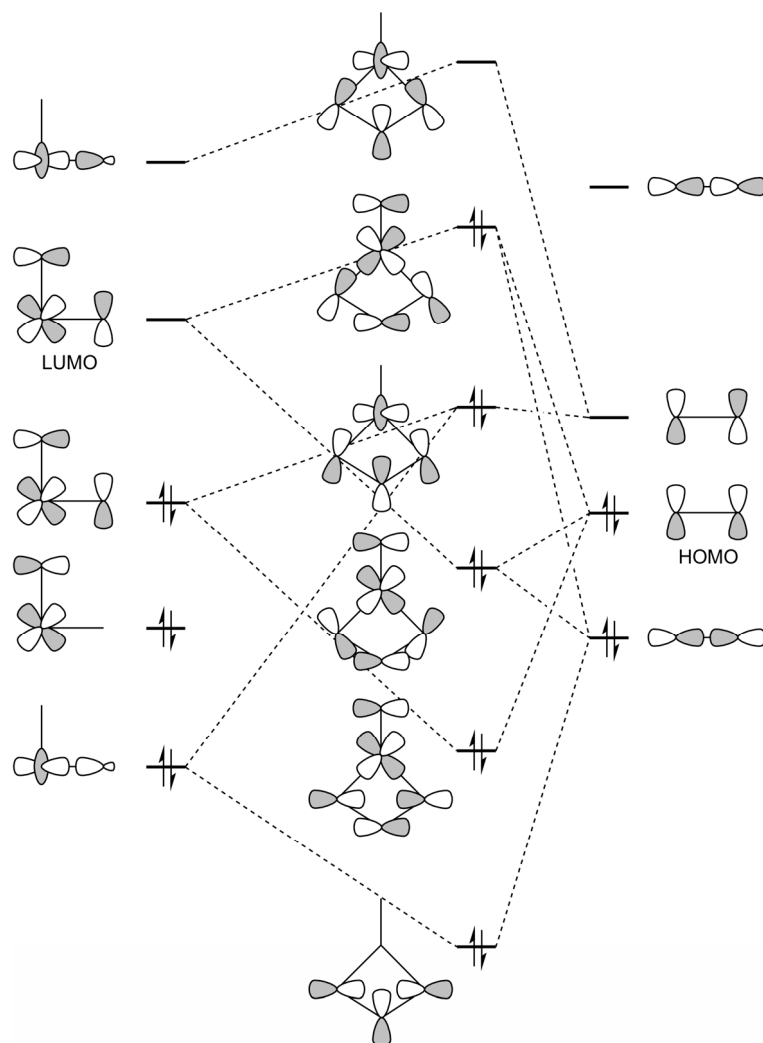


Fig. 38. Orbital interaction diagram for the formation of a metallacyclobutane on the COO face of a rotated pseudotetrahedral alkylidene complex [104].

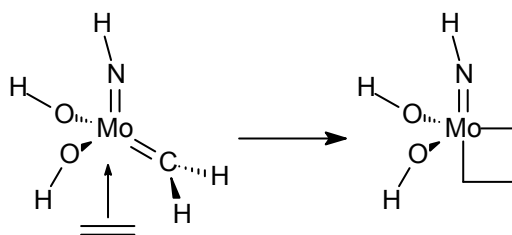


Fig. 39. The attack of the alkene at the COO face to form the metallacyclobutane [104].

Further studies on the addition of ethene to $\text{Mo}(\text{NH})(\text{CHR})(\text{OR}')_2$ ($\text{R} = \text{H}, \text{Me}$; $\text{R}' = \text{CH}_3, \text{CF}_3$) have been done by Wu and Peng [105]. They also investigated the possible faces of ethene addition to the catalyst (Fig. 40), the COO face and the CNO face.

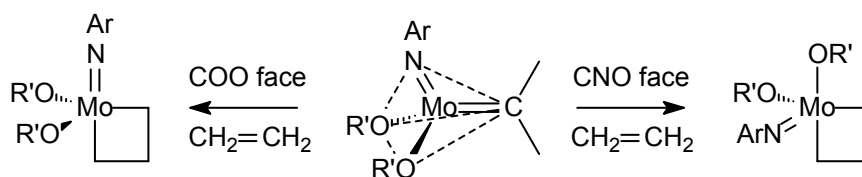


Fig. 40. The possible COO and CNO faces of addition [105].

Results indicated that the COO attack has a much higher activation energy due to the destabilization caused by the 90° rotation of the $M=C$ bond. Thus, it was concluded that olefin addition to the metal alkylidene takes place on the CNO face [105]. Furthermore, the transition structure of the CNO face attack was found to be a distorted TBP geometry with significant Mo-C and C-C bond formation [105]. In a follow-up paper [106] they investigated the ring-opening metathesis reaction of norbornadiene with molybdenum alkylidenes.

Monteyne and Ziegler [107] investigated the $[2+2]$ addition of ethene to the model catalyst $Mo(E)OCl_2$ with $E = S, Se, O, NH, PH, SiH_2$ and CH_2 (Fig. 41).

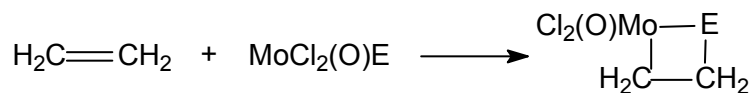


Fig. 41. $[2_\pi+2_\pi]$ cycloaddition of ethylene to the metal-ligand bonds, $Mo=E$, in $MoCl_2(O)E$ [107].

They found the feasibility of the addition to depend on the electronegativity of the heteroatom on the ligand E [107]. Less electronegative ligands lead to exothermic reactions and more electronegative ligands lead to endothermic reactions [107]. The addition of alkene to metal-carbene bonds is facile, whereas the addition to a $M=O$ bond is much less favorable [107].

Other computational studies on molybdenum complexes as metathesis catalysts [108, 109] and the nature of transition metal imido complexes [110,111] have also been done.

7. Summary

The results presented in this review show the viability of using computational and theoretical methods in the development of new alkene metathesis catalysts and to further elucidate the metathesis reaction mechanism. In most cases presented the modeling calculations were validated by experimental results. Only a few studies did an exclusive computational investigation. There is a clear trend in computational metathesis studies, whereby the initial studies calculated simplified model catalysts reacting with ethene. In later studies complete catalyst species are calculated combined with more complex alkenes. Only a handful of papers did a complete investigation of the whole catalytic cycle.

For computational metathesis to be truly effective in yielding results immediately applicable in catalyst design, the complete reaction system and catalytic cycle needs to be computed in future. Therefore, the solvent effect, reaction conditions, complete reagents and computational accuracy needs to be considered and incorporated. More computational studies directly correlated with experimental techniques, for example, NMR needs to be done. Since the advent of computational chemistry, computational alkene metathesis investigations made an important and irreplaceable contribution to alkene metathesis research.

References

- [1] R.H. Crabtree, *The Organometallic Chemistry of the Transition Elements*, fourth ed. Wiley, New York, 2005.
- [2] A.M. Rouhi, *Chem. Eng. News (Washington)* 80 (2002) 34.
- [3] J.C. Mol, *J. Mol. Cat. A* 213 (2004) 39.
- [4] C.P. Casey, T.J. Burkhardt, *J. Am. Chem. Soc.* 96 (1974) 7808.

- [5] T.J. Katz, J. McGinnis, *J. Am. Chem. Soc.* 97 (1975) 1592.
- [6] T.J. Katz, J. McGinnis, S. Hurwitz, *J. Am. Chem. Soc.* 98 (1976) 605.
- [7] R.R. Schrock, J.S. Murdzek, G.C. Bazan, J. Robbins, M. DiMare, M. O'Regan, *J. Am. Chem. Soc.* 112 (1990) 3875.
- [8] S.T. Nguyen, L.K. Johnson, R.H. Grubbs, *J. Am. Chem. Soc.* 114 (1992) 3974.
- [9] N. Calderon, H.Y. Chen, K.W. Scott, *Tetrahedron Lett.* 34 (1967) 3327.
- [10] Y. Chauvin, J. Herisson, *Makromol. Chem.* 141 (1971) 161.
- [11] R.R. Schrock, S. Rocklage, J. Wengrovius, G. Rupprecht, J. Fellmann, *J. Mol. Catal.* 8 (1980) 73.
- [12] J.P. Morgan, R.H. Grubbs, *Org. Lett.* 2 (2000) 3153.
- [13] C. Adlhart, P. Chen, *Angew. Chem. Int. Ed.* 41 (2002) 4484.
- [14] S.H. Hong, R.H. Grubbs, *J. Am. Chem. Soc.* 128 (2006) 3508.
- [15] T. Ritter, A. Hejl, A.G. Wenzel, T.W. Funk, R.H. Grubbs, *Organometallics* 25 (2006) 5740.
- [16] M. Jordaan, P. Van Helden, C.G.C.E. Van Sittert, H.C.M. Vosloo, *J. Mol. Catal. A* 254 (2006) 145.
- [17] M. Jordaan, H.C.M. Vosloo, *Adv. Synth. Catal.* 349 (2007) 184.
- [18] S.J. Malcolmson, S.J. Meek, E.S. Sattely, R.R. Schrock, A.H. Hoveyda, *Nature* 456 (2008) 933.
- [19] F.T.I. Marx, J.H.L. Jordaan, H.C.M. Vosloo, *J. Mol. Model.* 15 (2009) 1371.
- [20] I. Ibrahim, M. Yu, R.R. Schrock, A.H. Hoveyda, *J. Am. Chem. Soc.* 131 (2009) 3844.
- [21] K. Endo, R.H. Grubbs, *J. Am. Chem. Soc.* 133 (2011) 8525.
- [22] R.H. Grubbs, T.M. Trnka, M.S. Sanford, *Transition Metal-Carbene Complexes in Olefin Metathesis and Related Reactions*, in: H. Kurosawa, A. Yamamoto, (Eds.), *Current Methods in Inorganic Chemistry: Fundamentals of Molecular Catalysis*, Vol. 3. Elsevier, Amsterdam, 2003.
- [23] Y. Jean, *Molecular orbitals of transition metal complexes*. Oxford University Press, Oxford, 2005.
- [24] F. Mathey, A. Sevin, *Molecular Chemistry of the Transition Elements – An Introductory Course*. Wiley, Chichester, 1996.

- [25] G. Occhipinti, V.R. Jensen, *Organometallics* 30 (2011) 3522.
- [26] T.E. Taylor, M.B. Hall, *J. Am. Chem. Soc.* 106 (1984) 1576.
- [27] F.Z. Dörwald, *Metal Carbenes in Organic Synthesis*. Wiley-VCH, Weinheim, 1999.
- [28] R.R. Schrock, *J. Am. Chem. Soc.* 96 (1974) 6796.
- [29] E.O. Fischer, A. Maasböl, *Angew. Chem., Int Ed. Engl.* 3 (1964) 580.
- [30] J.C. Garrison, W.J. Youngs, *Chem. Rev.* 105 (2005) 3978.
- [31] S. Kotha, M.K. Dipak, *Tetrahedron* 68 (2012) 397.
- [32] S.F. Vyboishchikov, G. Frenking, *Chem. Eur. J.* 4 (1998) 1428.
- [33] J. Ushio, H. Nakatsuji, T. Yonezawa, *J. Am. Chem. Soc.* 106 (1984) 5892.
- [34] J. Ushio, H. Nakatsuji, T. Yonezawa, *J. Am. Chem. Soc.* 106 (1984) 5892.
- [35] G.O. Spessard, G.L. Miessler, *Organometallic Chemistry*. Prentice-Hall, 1997.
- [36] R.H. Grubbs, (Ed.), *Handbook of metatasis: Catalyst Development*, Vol. 2. Wiley-VCH, Weinheim, 2003.
- [37] R.R. Schrock, *Tetrahedron* 55 (1999) 8141.
- [38] M. Tlenkopatchev, S. Fomine, *J. Organomet. Chem.* 630 (2001) 157.
- [39] O. Eisenstein, R. Hoffman, *J. Am. Chem. Soc.* 103 (1981) 5582.
- [40] T.H. Upton, A.K. Rappé, *J. Am. Chem. Soc.* 107 (1985) 1206.
- [41] A.K. Rappé, W.A. Goddard III, *J. Am. Chem. Soc.* 104 (1982) 297.
- [42] F.U. Axe, J.W. Andzelm, *J. Am. Chem. Soc.* 121 (1999) 5396.
- [43] S.F. Vyboishchikov, M. Bühl, W. Thiel, *Chem. Eur. J.* 8 (2002) 3962.
- [44] S. Fomine, S.M. Vargas, M.A. Tlenkopatchev, *Organometallics* 22 (2003) 93.
- [45] F. Bernardi, A. Bottoni, G.P. Miscione, *Organometallics* 22 (2003) 940.
- [46] L. Cavallo, *J. Am. Chem. Soc.* 124 (2002) 8965.
- [47] C. Costabile, L. Cavallo, *J. Am. Chem. Soc.* 126 (2004) 9592.
- [48] W. Janse van Rensburg, P.J. Steynberg, W.H. Meyer, M.M. Kirk, G.S. Forman, *J. Am. Chem. Soc.* 126 (2004) 14332.
- [49] C. Adlhart, P. Chen, *J. Am. Chem. Soc.* 126 (2004) 3496.
- [50] C.H. Suresh, N. Koga, *Organometallics* 23 (2004) 76.
- [51] O.M. Aagaard, R.J. Meier, F. Buda, *J. Am. Chem. Soc.* 120 (1998) 7174.
- [52] B.F. Straub, *Angew. Chem. Int. Ed.* 44 (2005) 5974.

- [53] M. Vyboishchikov, W. Thiel, *Chem. Eur. J.* 11 (2005) 3921.
- [54] A.C. Tsipis, A.G. Orpen, J.N. Harvey, *Dalton Trans.* (2005) 2849.
- [55] A. Correa, L. Cavallo, *J. Am. Chem. Soc.* 128 (2006) 13352.
- [56] D. Benitez, E. Tkatchouk, W.A. Goddard III, *Chem. Commun.* (2008) 6194.
- [57] G. Occhipinti, H. Bjørsvik, V.R. Jensen, *J. Am. Chem. Soc.* 128 (2006) 6952.
- [58] K.B. Wiberg, *Tetrahedron* 24 (1968) 1083.
- [59] W. Janse van Rensburg, P.J. Steynberg, M.M. Kirk, W.H. Meyer, G.S. Forman, *J. Organomet. Chem.* 691 (2006) 5312.
- [60] B.F. Straub, *Adv. Synth. Catal.* 349 (2007) 204.
- [61] E.L. Dias, S.T. Nguyen, R.H. Grubbs, *J. Am. Chem. Soc.* 119 (1997) 3887.
- [62] S. Naumov, M.R. Buchmeiser, *J. Phys. Org. Chem.* 21 (2008) 963.
- [63] P.E. Romero, W.E. Piers, *J. Am. Chem. Soc.* 129 (2007) 1698.
- [64] C.E. Webster, *J. Am. Chem. Soc.* 129 (2007) 7490.
- [65] K. Getty, M.U. Delgado-Jaime, P. Kennepohl, *J. Am. Chem. Soc.* 129 (2007) 15774.
- [66] A. Poater, F. Ragone, A. Correa, L. Cavallo, *J. Am. Chem. Soc.* 131 (2009) 9000.
- [67] T. Weskamp, F.J. Kohl, W. Hieringer, D. Gleich, W.A. Herrman, *Angew. Chem. Int. Ed.* 38 (1999) 2416.
- [68] R.J. Meier, O.M. Aagaard, F. Buda, *J. Mol. Cat. A* 160 (2000) 189.
- [69] H. Jacobsen, *Dalton Trans.* 2006, 2214.
- [70] W.W. Schoeller, D. Schroeder, A.B. Rozhenko, *J. Organomet. Chem.* 690 (2005) 6079.
- [71] R.L. Lord, H. Wang, M. Vieweger, M. Baik, *J. Organomet. Chem.* 691 (2006) 5505.
- [72] I. Fernández, N. Lugan, G. Lavigne, *Organometallics* 31 (2012) 1155.
- [73] J.P. Foster, F. Weinhold, *J. Am. Chem. Soc.* 102 (1980) 7211.
- [74] P. Van der Gryp, S. Marx, H.C.M. Vosloo, *J. Mol. Cat. A* 355 (2012) 85.
- [75] F. Nuñez-Zarur, J. Poater, L. Rodríguez-Santiago, X. Solans-Monfort, M. Solà, M. Sodupe, *Comput. Theor. Chem.* 996 (2012) 57.
- [76] F. Nuñez-Zarur, X. Solans-Monfort, L. Rodríguez-Santiago, M. Sodupe,

- Organometallics 31 (2012) 4203.
- [77] I.W. Ashworth, I.H. Hillier, D.J. Nelson, J.M. Percy, M.A. Vincent, *Chem. Commun.* 47 (2011) 5428.
- [78] M.J. Lee, K.Y. Lee, J.Y. Lee, J.N. Kim, *Org. Lett.* 6 (2004) 3313.
- [79] S. Fomine, M. Tlenkopatchev, *J. Organomet. Chem.* 691 (2006) 5189.
- [80] I.H. Hillier, S. Pandian, J.M. Percy, M.A. Vincent, *Dalton Trans.* 40 (2011) 1061.
- [81] K.A. Burdett, L.D. Harris, P. Margl, B.R. Maughon, T. Mokhtar-Zadeh, P.C. Saucier, E.P. Wasserman, *Organometallics* 23 (2004) 2027.
- [82] S. Fomine, J.V. Ortega, M.A. Tlenkopatchev, *J. Mol. Cat. A* 236 (2005) 156.
- [83] S. Fomine, J.V. Ortega, M.A. Tlenkopatchev, *Organometallics* 24 (2005) 5696.
- [84] S. Fomine, J.V. Ortega, M.A. Tlenkopatchev, *J. Organomet. Chem.* 691 (2006) 3343.
- [85] S. Fomine, J.V. Ortega, M.A. Tlenkopatchev, *J. Mol. Cat. A* 263 (2007) 121.
- [86] S. Fomine, S. Gutierrez, M.A. Tlenkopatchev, *J. Organomet. Chem.* 694 (2009) 3287.
- [87] Y. Lu, F. Tournilhac, L. Leibler, Z. Guan, *J. Am. Chem. Soc.* 134 (2012) 8424.
- [88] S. Fomine, M.A. Tlenkopatchev, *J. Organomet. Chem.* 701 (2012) 68.
- [89] W.A. Goddard III, D. Benitez, *J. Am. Chem. Soc.* 127 (2005) 12218.
- [90] C. Adlhart, C. Hinderling, H. Baumann, P. Chen, *J. Am. Chem. Soc.* 122 (2000) 8204.
- [91] P. Hofmann, M.A.O. Volland, S.M. Hansen, F. Eisenträger, J.H. Gross, K. Stengel, *J. Organomet. Chem.* 66 (2000) 88.
- [92] J.N. Coalter, J.C. Bollinger, J.C. Huffman, U. Werner-Zwanziger, K.G. Caulton, E.R. Davidson, H. Gérard, E. Clot, O. Eisenstein, *New J. Chem.* 24 (2000) 9.
- [93] M. Jordaan, H.C.M. Vosloo, *Molecular Simulation* 34 (2008) 997.
- [94] I.C. Stewart, D. Benitez, D.J. O'Leary, E. Tkatchouk, M.W. Day, W.A. Goddard III, R.H. Grubbs, *J. Am. Chem. Soc.* 131 (2009) 1931.
- [95] X. Solans-Monfort, R. Pleixats, M. Sodupe, *Chem. Eur. J.* 16 (2010) 7331.
- [96] A. Fedorov, L. Batiste, A. Bach, D.M. Birney, P. Chen, *J. Am. Chem. Soc.* 133

- (2011) 12162.
- [97] I.T. Sabbagh, P.T. Kaye, *J. Mol. Struct.: THEOCHEM* 763 (2006) 37.
- [98] T.P.M. Goumans, A.W. Ehlers, K. Lammertsma, *Organometallics* 24 (2005) 3200.
- [99] A. Poater, X. Solans-Monfort, E. Clot, C. Copéret, O. Eisenstein, *J. Am. Chem. Soc.* 129 (2007) 8207.
- [100] X. Solans-Monfort, E. Clot, C. Copéret, O. Eisenstein, *J. Am. Chem. Soc.* 127 (2005) 14015.
- [101] M. Vasiliu, S. Li, A.J. Arduengo III, D.A. Dixon, *J. Phys. Chem. C.* 115 (2011) 12106.
- [102] T.R. Cundari, M.S. Gordon, *Organometallics* 11 (1992) 55.
- [103] E. Folga, T. Ziegler, *Organometallics* 12 (1993) 325.
- [104] H.H. Fox, M.H. Schofield, R.R. Schrock, *Organometallics* 13 (1994) 2804.
- [105] Y. Wu, Z. Peng, *J. Am. Chem. Soc.* 119 (1997) 8043.
- [106] Y. Wu, Z. Peng, *Inorg. Chim. Acta.* 345 (2003) 241.
- [107] K. Monteyne, T. Ziegler, *Organometallics* 17 (1998) 5901.
- [108] A.K. Rappé, W.A. Goddard III, *J. Am. Chem. Soc.* 102 (1980) 5114.
- [109] A.K. Rappé, W.A. Goddard III, *J. Am. Chem. Soc.* 104 (1982) 448.
- [110] T.R. Cundari, M.S. Gordon, *J. Am. Chem. Soc.* 113 (1991) 5231.
- [111] T.R. Cundari, *J. Am. Chem. Soc.* 114 (1992) 7879.